PLASTICITY IN VISUAL PERCEPTUAL LEARNING

BY

JI WON BANG

M.A., BROWN UNIVERSITY, 2014

M.A., BOSTON UNIVERSITY, 2012

B.A., KOREA UNIVERSITY, 2008

SUBMITTED IN PARTIAL FULFILLMENT OF THE REQUIREMENTS FOR THE DEGREE OF DOCTOR OF PHILOSOPHY IN THE DEPARTMENT OF COGNITIVE, LINGUISTIC & PSYCHOLOGICAL SCIENCES AT BROWN UNIVERSITY

PROVIDENCE, RHODE ISLAND

May 2016

This thesis by Ji Won Bang is accepted in its present form
by the Department of Cognitive, Linguistic & Psychological Sciences as satisfying the thesis requirement for the degree of Doctor of Philosophy.

Date _____ _____

Takeo Watanabe, Advisor

Recommended to the Graduate Council

Date _____ _____

Joo-Hyun Song, Reader

Date _____ _____

Yuka Sasaki, Reader

Approved by the Graduate Council

Date _____ _____

Peter M. Weber, Dean of the Graduate School

CURRICULUM VITA

Ji Won Bang

Department of Cognitive, Linguistic & Psychological Sciences
Brown University
190 Thayer Street, Providence, RI 02912
Ji_Won_Bang@brown.edu
(401)338-5615

Education

2012 – 2015	**Brown University,** Providence, RI Ph.D in Psychology
2010 – 2012	**Boston University,** Boston, MA M.A. in Psychology
2003 – 2008	**Korea University,** Seoul, South Korea B.A. in Psychology

Awards and Honors

2015	Student Travel Award, Vision Sciences Society, St. Pete Beach, FL
2012	Hot topic, Society for Neuroscience, San Diego, CA
2011 – 2012	Dean's Scholarship, Boston Univ., Boston, MA
2009	Brain Korea 21 Scholarship, Korea Univ., Seoul, South Korea
2003 – 2004	Semester High Honors Scholarship, Korea Univ., Seoul, South Korea

Research Experience

2012 – present	**Brown University** Research Assistant; Advisor: Prof. Takeo Watanabe
2010 – 2012	**Boston University** Research Assistant; Advisor: Prof. Takeo Watanabe
2010 – 2012	**Massachusetts General Hospital - Martinos Center for Biomedical Imaging** Research Assistant; Advisor: Prof. Yuka Sasaki
2009	**Korea University** Research Assistant; Advisor: Prof. Hackjin Kim

Publications

Peer-reviewed publications:

1. **Bang, J. W.**, Khalilzadeh, O., Hamalainen, M., Watanabe, T., & Sasaki, Y. (2014). *Location specific sleep spindle activity in the early visual areas and perceptual learning,* Vision research 99:162-171
2. Tamaki, M., **Bang, J. W.**, Watanabe, T., & Sasaki, Y. (2014). *The first-night effect suppresses the strength of slow-wave activity originating in the visual areas during sleep,* Vision research 99:154-161.
3. Sung, Y. S., Lee, H. J., Park, H. Y., **Bang, J. W.** (2009). Neural consequences of delayed gratification of curiosity, The Korean Journal of Advertising 20:43-58

Manuscripts in progress:

1. **Bang, J. W.**, Watanabe, T., & Sasaki, Y., *Effect of reactivation in visual perceptual learning* (In preparation)
2. Tamaki, M., **Bang, J. W.**, Watanabe, T., & Sasaki, Y., *Asymmetrical sleep in human in association with the first-night effect* (Submitted)
3. **Bang, J. W.**, Shibata, K., Watanabe, T., & Sasaki, Y., *Neural mechanism of reactivation of consolidated perceptual learning revealed by the concentration of excitatory and inhibitory neurotransmitters* (In preparation)
4. Shibata, K., **Bang, J. W.**, Machizawa, M. G., Walsh, E. G., Chang, L., Berard, A., Tan, Q., Sasaki, Y., & Watanabe, T., *The neural mechanism of stabilization of perceptual learning revealed by the concentration of excitatory and inhibitory neurotransmitters* (In preparation)

Abstracts and conference proceedings:

1. **Bang, J. W.**, Shibata, K., Watanabe, T., Sasaki, Y., *Neural mechanism of reactivation of consolidated perceptual learning revealed by the concentration of excitatory and inhibitory neurotransmitters,* Annual Meeting of the Vision Sciences Society, St. Pete Beach, FL, 2015
2. Shibata, K., Machizawa, M. G., Walsh, E., **Bang, J. W.**, Chang, L., Berard, A., Tan, Q., Sasaki, Y., Watanabe, T., *The neural mechanism of stabilization of perceptual learning revealed by the concentration of excitatory and inhibitory neurotransmitter,* Annual Meeting of the Vision Science Society, St. Pete Beach, FL, 2015
3. **Bang, J. W.**, Watanabe, T., Sasaki, Y., *Role of sleep spindle in early visual areas and perceptual learning,* Annual Meeting of the Society for Neuroscience, San Diego, CA, 2013
4. Tamaki, M., **Bang, J. W.**, Watanabe, T., Sasaki, Y., *Altered slow-wave activity in the default mode network during sleep associated with the first-night effect,* Annual Meeting of the Society for Neuroscience, San Diego, CA, 2013
5. **Bang, J. W.**, Watanabe, T., Sasaki, Y., *Role of sleep spindle in early visual areas and perceptual learning,* Annual Meeting of the Sleep, Baltimore, MD, 2013

6. Tamaki, M., **Bang, J. W.**, Watanabe, T., Sasaki, Y., *Altered slow-wave activity in the default mode network during non-rapid eye movement sleep associated with the first-night effect in combination of MEG and MRI,* Annual Meeting of the Sleep, Baltimore, MD, 2013
7. **Bang, J. W.**, Sato, S., Watanabe, T., Sasaki, Y., *Reconsolidation in visual perceptual learning,* Annual Meeting of the Vision Sciences Society, Naples, FL, 2013
8. Tamaki, M., **Bang, J. W.**, Watanabe, T., Sasaki, Y., *Modification of spontaneous oscillatory activity in the visual cortex during non-rapid eye movement sleep associated with adaptation process to a first-night sleep environment,* Annual Meeting of the Vision Sciences Society, Naples, FL, 2013
9. **Bang, J. W.**, Khalilzadeh, O., Wakeman, D., Tamaki, M., Hamalainen, M., Watanabe, T., Sasaki, Y., *MEG slow activity in V1 during sleep and perceptual learning,* Annual Meeting of the Vision Sciences Society, Naples, FL, 2012

Teaching Experience

Brown University

2014 Fall	Teaching Assistant*, CLPS 0900 Quantitative Methods in Psychology*
2014 Summer	Instructor*, CEBN 0924 Visual Consciousness*
2014 Spring	Teaching Assistant*, CLPS 0500 Perception and Mind*
2013 Fall	Teaching Assistant*, CLPS 0020 Approaches to the Mind: Introduction to Cognitive Science*
2013 Spring	Teaching Assistant*, CLPS 0510 Perception, Illusion, and the Visual Arts*

Other Training, and Certification

2014	**Brown University – MRI Research Facility (MRF)** MRF Level-3 certificate (Scanner Operator)
2013 - 2014	**Brown University – Sheridan Center for Teaching and Learning** Sheridan Teaching Seminar – Certificate 1 Program
2013	**Massachusetts General Hospital – Martinos Center for Biomedical Imaging** FreeSurfer workshop

ACKNOWLEDGEMENTS

I could complete this thesis because the people that I met helped me move forward to the next step, whenever I faced challenge. Especially, I thank my advisor, Takeo Watanabe and Yuka Sasaki for giving me the opportunity to study vision science under their supervision. With their help, I could walk into the research field and learn the invaluable lessons that I could not have in other places. I am also thankful to my dissertation committee, Joo-Hyun Song for giving me encouragement and advice on my way to here.

I thank the current and the past members of Laboratory for Cognitive and Perceptual Learning, including Kazuhisa Shibata, Masako Tamaki, Dongho Kim, Hoon Choi, Li-Hung Chang, Maro Machizawa, Qingleng Tan, Aaron V. Berard, Tren Huang, Charles Liu, Omid Khalilzadeh, Daniel G. Wakeman, Erika Scilipoti, Matthew S. Cain, Jeffrey Bower, Akiko Norton, and Nozomi Ito.

Finally, I owe my deepest thanks and love to my family. My family gave me unconditional love and support in every step. I have to admit that without them, I cannot stand here today.

TABLE OF CONTENTS

LIST OF TABLES

LIST OF FIGURES

LIST OF ABBREVIATIONS

AASM	American academy of sleep medicine
BDNF	brain-derived neurotropic factor
BOLD	blood-oxygen-level-dependent
E/I ratio	ratio of excitatory to inhibitory signals
ECG	electrocardiogram
EEG	electroencephalogram
EMG	electromyogram
EOG	electrocardiogram
fMRI	functional magnetic resonance imaging
FNE	first night effect
GABA	γ-aminobutyric acid
HPI	head position indicators
LTD	long-term depression
LTP	long-term potentiation
MEG	magnetoencephalography
MNE	minimum norm estimate
MRI	magnetic resonance imaging
MRS	magnetic resonance spectroscopy
NREM	non-rapid eye movement
PSG	polysomnography
REM	rapid eye movement
ROI	regions of interest
SOA	stimulus-to-mask onset asynchrony
SSS	Stanford sleepiness scale
SWS	slow-wave sleep
TDT	texture discrimination task
VPL	visual perceptual learning

1. Chapter 1: Introduction

1.1 Visual perceptual learning (VPL)

Visual perceptual learning (VPL) refers to a long-term performance enhancement on a visual task as a result of repeated visual training (Sasaki, Nanez & Watanabe, 2010). VPL is regarded as a manifestation of brain plasticity, especially for those who have gone through a critical period of perceptual development (Sasaki, Nanez & Watanabe, 2010). Therefore, VPL is thought to be a critical tool that can help identify how the adult visual system can change after the critical period.

1.2 Specificity of VPL and plasticity in visual cortex

VPL is highly specific to the visual location of the trained stimulus (Crist et al., 1997; Fahle & Edelman, 1993; Fiorentini & Berardi, 1980; Karni & Sagi, 1991; McKee & Westheimer, 1978; Poggio, Fahle & Edelman, 1992; Sagi & Tanne, 1994; Shiu & Pashler, 1992) and features of the stimulus (Ball & Sekuler, 1987; Fiorentini & Berardi, 1980; Koyama, Harner & Watanabe, 2004; Poggio, Fahle & Edelman, 1992; Schoups et al., 2001; Vaina et al., 1998; Watanabe et al., 2002). These perceptual specificities suggest that neuronal changes associated with VPL occur within visual areas, which are highly organized with respect to location and feature. Previous studies have investigated the possible cortical sites of VPL and reported neuronal changes in the lowest areas of visual cortex, such as V1 (Hua et al., 2010; Li, Piech & Gilbert, 2004; Schoups et al., 2001; Schwartz, Maquet & Frith, 2002; Shibata et al., 2011) or higher-level visual cortical areas such as V4 (Adab & Vogels, 2011; Raiguel et al., 2006; Yang & Maunsell,

2004) and MT (Gu et al., 2010; Zohary et al., 1994). It should be noted, however, that the location specificity in VPL has become controversial in some cases (Xiao et al., 2008; Zhang et al., 2010a; Zhang et al., 2010b) and sensory adaptation plays a critical role in location specificity (Harris, Gliksberg & Sagi, 2012).

1.3 Consolidation process of VPL

It has been suggested that there is temporal dynamics of consolidation in the development of VPL after the offset of visual training. Generally, the consolidation process is defined as a process whereby the memory is transformed into a stable and enduring form with a passage of time after encoding (McGaugh, 2000; Squire & Davis, 1981). In VPL, this temporal dynamics of consolidation consists of at least two phases according to previous findings: wake-dependent stabilization, and sleep-dependent enhancement (Sasaki, Nanez & Watanabe, 2010). After the visual training, VPL becomes stabilized and enhanced during subsequent wakefulness and sleep periods, respectively. In the following sections (Chapter 1.3.1 & 1.3.2), the findings in the wake-dependent stabilization and sleep-dependent enhancement of VPL are introduced. In addition, we discuss another possible temporal dynamics in VPL, which are reactivation and reconsolidation (Chapter 1.3.3), based on the findings in other general memory domains.

1.3.1 Wake-dependent stabilization of VPL

Wake-dependent consolidation is known to make VPL stable. Previous studies indicate that if the first learning is immediately followed by the second competing task, the second learning interferes with the consolidation of the first learning (Seitz et al., 2005; Yotsumoto et al., 2009a). As a consequence, performance of the firstly learned task is not enhanced on the next day. In contrast, when the second learning is provided after one hour since the first learning, interference does not occur and thus performance of the firstly learned task improves on the next day (Seitz et al., 2005). Such interference effect within a limited time window is regarded as the evidence of changes in stability of VPL during wakefulness: VPL becomes stabilized during wakefulness.

1.3.1.1 E/I ratio – a possible underlying neural mechanism of wake-dependent stabilization in VPL

Recently, it has been proposed that the ratio between excitatory and inhibitory signals (E/I ratio) regulates the plastic potential of the brain directly (Bavelier et al., 2010; Hensch, 2005; Morishita & Hensch, 2008). Particularly, the relationship between the brain plasticity and E/I ratio has been studied extensively in the critical period plasticity of vision. During pre-critical period for ocular dominance, the cortical circuits are dominated by excitation. However, as the inhibitory connections are developed later than excitatory connections, the E/I circuit balance changes and the critical period starts. Accumulating studies support that this late-developing E/I ratio change plays a critical role in initiating the critical period of vision. For example, when the maturation of γ-

aminobutyric acid (GABA), which is the primary inhibitory neurotransmitter is disrupted by deletion of Gad65 (Hensch et al., 1998) or dark-rearing from birth (Chen, Yang & Mower, 2001; Fagiolini et al., 2003; Morales, Choi & Kirkwood, 2002; Mower, 1991), the onset of visual critical period is delayed. In contrast, the critical period can be triggered prematurely if GABA transmission is enhanced via benzodiazepines (Fagiolini et al., 2004; Fagiolini & Hensch, 2000; Iwai et al., 2003) or the maturation of the inhibitory interneurons is accelerated through excess brain-derived neurotropic factor (BDNF) expression (Hanover et al., 1999; Huang et al., 1999).

Once the critical period is passed, the established brain loses its heightened plasticity. One example is that the effect of the abnormal visual input on the visual acuity varies greatly depending on when this perturbation occurs. The abnormal visual input caused by congenital cataracts, misaligned eyes, or experimental monocular deprivation during infancy leads to loss of vision in the amblyopic eye and disrupts the maturation of ocular dominance columns (Lewis & Maurer, 2009). However, if this abnormality occurs in the adulthood, its effects are smaller or nonexistent (Hubel & Wiesel, 1970). It indicates that the potential plasticity of the brain is reduced as the development proceeds.

Surprisingly, recent researches found that the plastic potential of brain can be restored even in the adulthood by resetting E/I ratio. A direct pharmacological manipulation that decreases intracortical inhibition is found to enhance visual plasticity in the adult amblyopic animals (Harauzov et al., 2010). A dark exposure manipulation followed by reverse deprivation also restores visual plasticity in the adult animal's amblyopic eye (He et al., 2007; Montey & Quinlan, 2011). Notably, this dark exposure is known to reduce intracortical inhibition. In addition, reverse suture coupled with enriched

environment (Sale et al., 2007) or fluoxetine treatment (Maya-Vetencourt et al., 2008) in adult amblyopic animals promoted recovery of visual functions in the amblyopic eye. This recovery from amblyopia was accompanied by reduced GABAergic inhibition. However, when benzodiazepines, which enhances GABAergic inhibition was cortically administered, these effects were prevented. These findings imply that the visual plasticity can be reopened by a reduction in GABAergic inhibition in the adulthood.

In human studies, the changes in the excitatory or inhibitory signals were studied in association with learning. Previous human studies suggest that the degree of learning is associated with increase of excitatory signals or decrease of inhibitory signals in a brain region involved in learning (Clark et al., 2012; Clark et al., 2011; Kim et al., 2014; Stagg, Bachtiar & Johansen-Berg, 2011). The excitatory and inhibitory signals in the brain can be measured by magnetic resonance spectroscopy (MRS) (Stagg, Bachtiar & Johansen-Berg, 2011). Considering that learning entails plasticity in the brain, these findings imply that the brain's plastic potential is governed by the E/I ratio. However, it should be noted that previous human studies examined either excitatory or inhibitory signals only, but not the E/I ratio.

1.3.1.2 Problem statement

The literature review on E/I ratio suggests that the underlying neural mechanism of wake-dependent stabilization in VPL could be associated with the changes in E/I ratio in early visual areas. This question has not been examined yet despite of the accumulating behavioral evidence showing that VPL is stabilized during the subsequent

wakefulness. If the underlying mechanism of wake-dependent stabilization is associated with E/I ratio changes in early visual areas, it could suggest that the mechanism of stabilization of VPL in adult's visual system is similar to the mechanism of a visual critical period in early life.

1.3.2 Sleep-dependent enhancement of VPL

Sleep-dependent consolidation process leads to performance improvement in VPL. Previous researches demonstrate that sleep plays a critical role in performance improvement of VPL (Bang et al., 2013; Gais et al., 2000; Karni & Sagi, 1993; Korman et al., 2007; Mednick, Nakayama & Stickgold, 2003; Stickgold, James & Hobson, 2000; Stickgold et al., 2000; Tamaki et al., 2013; Yotsumoto et al., 2009b). Karni & Sagi (1993) have shown that learning of a texture discrimination task (TDT) does not improve after as much as eight hours of wakeful rest, but improves significantly after a full night sleep. Notably, research has shown that sleep must occur within 30 hours of practice in order for subsequent performance improvements to develop (Stickgold, James & Hobson, 2000). Sleep is a multifaceted process with distinct neuronal activity patterns nested within each sleep stage. Thus, it has been assumed that each sleep stage plays a different role in the consolidation of VPL (Stickgold et al., 2000).

1.3.2.1 Sleep stages and its relevance to VPL

Sleep can be broadly categorized into non-rapid eye movement (NREM) sleep and rapid eye movement (REM) sleep: NREM sleep can be further divided into stage 2 and slow-wave sleep (SWS). According to Gais et al. (2000), the neuronal processes related to the early sleep period, which contains an abundance of NREM sleep and very little REM sleep, facilitate consolidation of VPL, whereas the later sleep period, which has abundant REM sleep, does not facilitate consolidation, if the later sleep period alone occurs. In addition, Yotsumoto et al. (2009) has shown that brain activity in the trained region of V1 during NREM sleep is significantly greater after training compared to before training. Interestingly, the brain activity within the trained region of V1 observed during NREM sleep was highly correlated with later performance improvements on the trained task. These studies suggest that NREM sleep plays a crucial role in the development of performance improvements. Notably, the latter study indicates that the consolidation processes of NREM sleep occur specifically within trained region of early visual areas.

1.3.2.2 Two models

There are two leading models which attempt to explain the neuronal mechanism of consolidation during sleep: an active system consolidation model (Born, Rasch & Gais, 2006; Born & Wilhelm, 2012; Hasselmo, 1999; Rasch et al., 2007) and a synaptic homeostasis model (Tononi & Cirelli, 2003, 2006). Please note that these models may or

may not explain the sleep-dependent enhancement in VPL to the fullest because they are not developed based on VPL.

1.3.2.2.1 Active system consolidation model

The active system consolidation model assumes that memory traces that are involved in learning are reactivated and redistributed during subsequent NREM sleep, so that synaptic connections in the neocortex are strengthened (Born, Rasch & Gais, 2006; Born & Wilhelm, 2012; Hasselmo, 1999; Rasch et al., 2007). According to this model, the memory replay and redistribution processes are mediated by sleep spindle and slow-wave activity, which are the most prominent features of sleep stage 2 and SWS, respectively (Born, Rasch & Gais, 2006; Born & Wilhelm, 2012). Sleep spindles are generated from the thalamic nucleus reticularis and spread to the entire neocortex (Steriade, McCormick & Sejnowski, 1993), whereas slow-waves are primarily generated in the neocortex and extend to other areas such as the hippocampus and thalamus (Buzsaki & Draguhn, 2004; Steriade, 1999). Experiments have demonstrated that spike trains similar to spindle activity induce long-term potentiation (LTP) in cortical neurons (Rosanova & Ulrich, 2005). Research in humans has shown that spindle activity increases after intense learning of a declarative word pair task (Gais et al., 2002; Molle et al., 2009; Schabus et al., 2004; Schmidt et al., 2006) and a procedural motor task (Fogel & Smith, 2006; Morin et al., 2008). In addition, it has been shown that performance improvements on a trained task correlate with spindle activity in cortical areas primarily associated with the task: for example, the parietal cortex and a visuospatial task (Clemens, Fabo & Halasz,

2006), the prefrontal cortex and a word pair task (Clemens, Fabo & Halasz, 2005), and the motor cortex after a finger tapping task (Nishida & Walker, 2007). Slow-wave activity is also thought of as a signature of consolidation during sleep. Slow-waves temporally bind neuronal activity, including sleep spindles and ripples into depolarizing up-states during which neurons' firing rates increase to a level similar to a waking state (Steriade, 2006). Previous studies have shown that ripples and spindles nested in depolarizing up-states of slow-waves support LTP (Buzsaki, Haas & Anderson, 1987; King et al., 1999; Rosanova & Ulrich, 2005). However, it should be noted that the role of slow-waves is still controversial; it has been shown that slow-waves with T-type Ca^{2+} influx lead to long-term depression (LTD) (Czarnecki, Birtoli & Ulrich, 2007).

1.3.2.2.2 Synaptic homeostasis model

On the other hand, the synaptic homeostasis model proposes that global synaptic downscaling, which occurs during sleep, generates performance improvements after sleep as a by-product, and does not necessarily support the existence of specific consolidation processes during sleep (Tononi & Cirelli, 2003, 2006). According to this theory, synapses become potentiated as information is encoded in the brain during the waking state. Sleep then globally downscales synaptic strength to an energetically sustainable level. As a result, weak synaptic connections are removed, and the remaining relatively strong synaptic connections are preserved. This process improves the signal-to-noise ratio of the encoded information and leads to memory enhancement. Slow-waves are assumed to be related to synaptic downscaling because slow-waves associated with Ca^{2+} channel

activation induce LTD (Czarnecki, Birtoli & Ulrich, 2007). There is some evidence to support the synaptic homeostasis model. A local increase in slow wave activity was found in cortical motor areas during sleep after a motor learning task, and this activity was correlated with performance gain (Huber et al., 2004). Subsequent research showed that slow wave activity was reduced when information encoding was prevented (Huber et al., 2006). This indicates that changes in synaptic strength are directly related to slow wave activity: greater synaptic strength is associated with greater downscaling.

1.3.2.3 Problem statement

It remains to be seen whether sleep spindles and/or slow-waves are involved in the consolidation of VPL, which is thought to involve early visual areas (Hua et al., 2010; Li, Piech & Gilbert, 2004; Schoups et al., 2001; Schwartz, Maquet & Frith, 2002; Shibata et al., 2011). If it can be found which oscillatory activity is involved in the consolidation of VPL, it may shed a light on which model among active system consolidation model and synaptic homeostasis model explains the underlying mechanism of consolidation of VPL.

1.3.3 Reactivation and reconsolidation processes of VPL

1.3.3.1 Evidence from other memory domains

It is well known that once VPL goes through wake-dependent and sleep-dependent consolidations, VPL is transformed into stable and long-lasting form, thus

rarely goes back to the fragile state again. However, in the other memory domains besides VPL, it has been shown that memory retrieval can change the existing memory into a fragile state once again, thus making it susceptible to interference from competing tasks (Chan & LaPaglia, 2013; Forcato et al., 2007; Hupbach et al., 2007; Walker et al., 2003). Memory retrieval is assumed to *reactivate* the relevant memory trace that was once consolidated (Chan & LaPaglia, 2013; Forcato et al., 2007; Hupbach et al., 2007; Walker et al., 2003). When the memory is rendered vulnerable as a result of retrieval/reactivation, following new information can impair (Walker et al., 2003) or modify the vulnerable memory to incorporate new learning (Chan & LaPaglia, 2013; Forcato et al., 2007; Hupbach et al., 2007).

Notably, reactivated memory is shown to go through another critical temporal dynamics; that is, reconsolidation. Reactivated memory becomes reconsolidated during a certain time window. This time window of reconsolidation process seems to vary from one to six hours depending on the types of memory (Nader, Schafe & Le Doux, 2000; Schiller et al., 2010; Seitz et al., 2005; Xue et al., 2012). Previous studies demonstrate that once the reactivated memory is reconsolidated during this time window, the following new information does not interfere with the old memory any more (Nader, Schafe & Le Doux, 2000; Schiller et al., 2010; Seitz et al., 2005; Xue et al., 2012). This time window is thought to be related to the time needed for protein synthesis in neurons, which is associated with both consolidation and reconsolidation processes (Davis & Squire, 1984; Flexner, Flexner & Stellar, 1965; Goelet et al., 1986).

1.3.3.2 Problem statement

Despite the accumulating evidence of reactivation and reconsolidation processes in various memory domains, it has not been studied yet whether the reactivation and reconsolidation process also exists in VPL. Theoretically, reactivation of VPL is possible via brief visual task that was trained before. However, it is unknown whether this reactivation of VPL would change previously consolidated VPL to a fragile state once again so that the following new task may interfere with the reactivated VPL.

If reactivation makes previously consolidated VPL into fragile state again, its underlying mechanisms might be associated with the E/I ratio changes in early visual areas. It is because the E/I ratio is proposed as a key factor that regulates the plastic potential of the brain during the critical period (Bavelier et al., 2010; Hensch, 2005; Morishita & Hensch, 2008). It is important to address this question because it can reveal a common mechanism that governs the plasticity and stability of the visual system across adulthood and early life.

1.4 Research aims

Based on the literature reviewed and the problem statements mentioned above, this dissertation research aims to address five questions: (1) Is E/I ratio change associated with the underlying mechanism of wake-dependent stabilization in VPL? (2) Which oscillatory activity is involved in the sleep-dependent enhancement of VPL during the first cycle of NREM sleep? (3) Does reactivation make already consolidated VPL fragile again? (4) Is E/I ratio change associated with the underlying mechanism of reactivation in

VPL? (5) Is the reactivation a general process in VPL regardless of the task? To probe these questions, we conducted systematic observations into behavioral experiments and functional brain activity related with VPL.

2. Chapter 2: Wake-dependent stabilization of VPL

2.1 Introduction

The current study under Chapter 2 aims to investigate if the underlying mechanism of wake-dependent stabilization in VPL is associated with the E/I ratio changes in the early visual cortex. In order to examine this, first we tested if VPL is fragile against interference shortly after training but becomes stabilized with a passage of time in the following behavioral experiment (Chapter 2.2). Then we examined how the E/I ratio changes in the early visual cortex after training in the following imaging experiment (Chapter 2.3).

2.2 VPL is stabilized during subsequent wakefulness

2.2.1 Methods

2.2.1.1 Subjects

Twenty-four healthy subjects (18 to 34 years old) with no use of medication participated in the experiment. All subjects had normal or corrected-to-normal vision. They kept regular wake and sleep pattern during experimental days. All subjects were informed of the purpose and the procedures of the experiment and gave written informed consent, which was approved by the Institutional Review Board of Brown University where the experiment was conducted.

2.2.1.2 Experimental design

To examine if VPL is unstable immediately after training but becomes stable with a passage of time, we used orientation detection task with two orientations, 10 and 70 degree. Two orientations were randomly assigned to orientation A (firstly trained orientation) and B (secondly trained orientation) across subjects. In addition, subjects were randomly assigned to either short or long interval group. In the short interval group, there was 30 minutes time interval between the training of orientation A and new training of orientation B, whereas in the long interval group, there was 3.5 hours interval. The purpose of having two groups was to test if the stability of VPL changes as a function of time since training.

The entire behavioral experiment consisted of two consecutive days (Figure 1). On the first day, subjects were given a brief test session consisting of one block per orientation. The purpose of the test session was to measure the initial threshold for each orientation. After the test session, subjects were provided with the training session of orientation A consisting of 8 blocks. In the short interval group, another 8 blocks of training on orientation B was provided 30 minutes after the training of orientation A. On the other hand, in the long interval group, new training on orientation B was given 3.5 hours after the training on orientation A.

On the second day, subjects were provided with test sessions of orientation A and B. By comparing the performance on orientation A between the first and the second day, we can examine if new learning of orientation B interfered with VPL of orientation A.

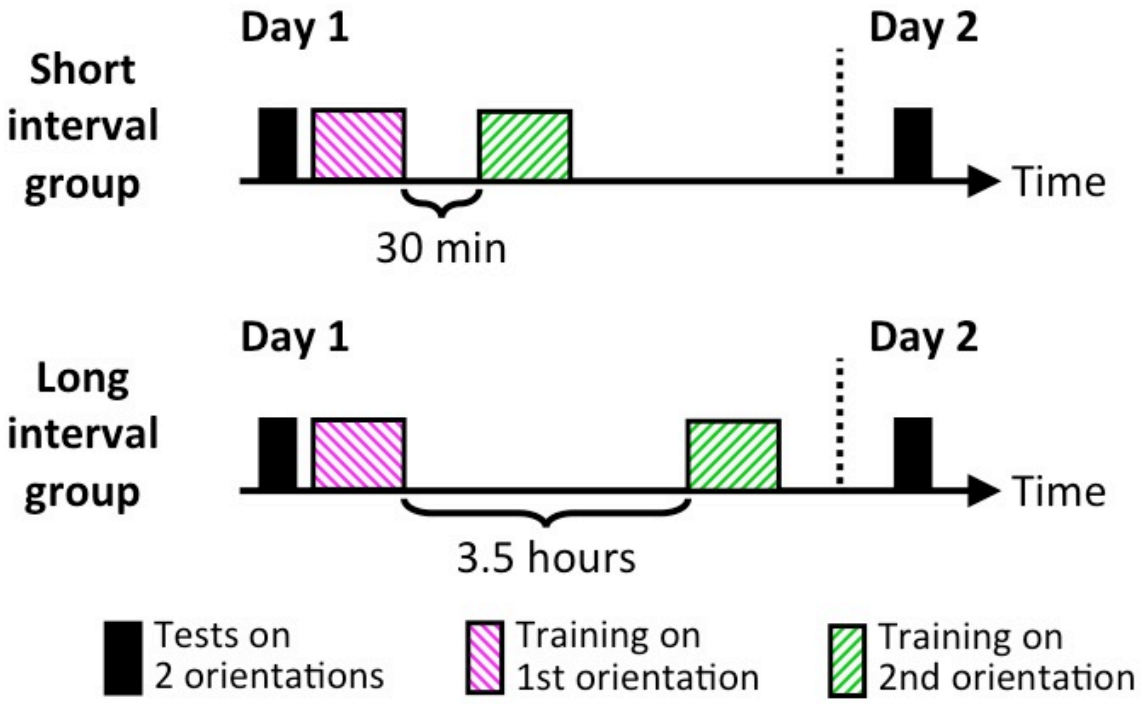

Figure 1. Experimental procedure.

2.2.1.3 Gabor stimulus

Gabor patches with one orientation (contrast = 100%, spatial frequency = 1 cycle/degree, sigma of its Gaussian filter = 2.5 degree, random spatial phase) were presented within an annulus covering 0.75 to 5 degree from the center of the screen. Noise pattern generated from a sinusoidal luminance distribution was superimposed on the Gabor patches and it yielded a certain signal to noise (S/N) ratio.

2.2.1.4 Orientation detection task

Subjects performed a 2-interval-forced-choice (2IFC) orientation detection task (Figure 2). In one stimulus, the Gabor patch was presented with a certain S/N ratio. In the other stimulus, only the noise pattern (0% S/N ratio) was presented. The order of two stimuli was determined randomly. During the entire task, subjects were asked to fix their eyes at the central white dot on a gray disk (0.75 degree). Each trial started with 500-ms fixation period. After the fixation period, two stimuli intervals were presented for 50 ms in order, which were separated by a 300-ms blank period. Then, participants were asked to determine where the Gabor patch appeared among two stimuli intervals by pressing buttons on a key pad. There was no feedback for the response

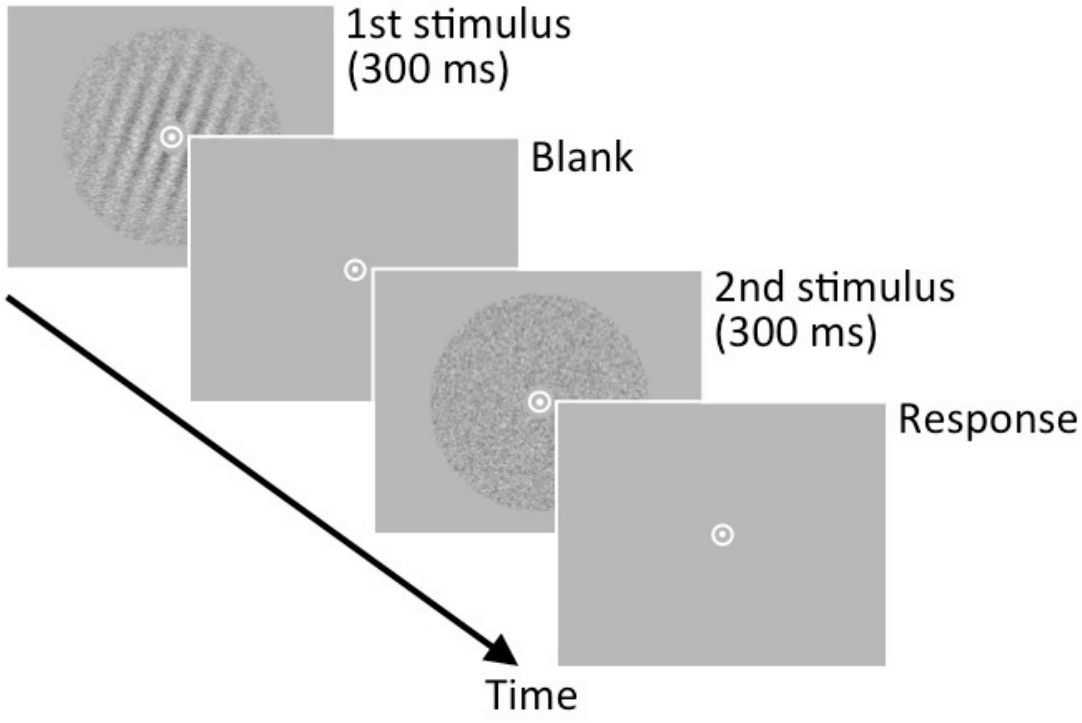

Figure 2. Orientation detection task.

2.2.1.5 Threshold measurement

Each subject's threshold S/N ratio in each block was determined by 2-down 1-up staircase rule. This method yields 70.7% accuracy rate. Each block started with 25% S/N ratio and terminated after 10 reversals. Each block consisted of 30-40 trials and took 1-2 minutes approximately. We took the geometric mean of the last 6 reversals in one block as a threshold S/N ratio per orientation (Xiao et al., 2008).

2.2.1.6 Behavioral test and training sessions

In the behavioral test session, subjects were given one block per orientation. The order of the two orientations was randomly chosen. During the behavioral training session, subjects were provided with 8 blocks of one orientation.

2.2.2 Results

To test if VPL of orientation A is fragile against interference immediately after training, but becomes stabilized by 3.5 hours after the training, we computed the threshold % change of orientation A across the first and the second day per subject:

$$\text{Threshold \% change}_{\text{day1 \& 2}} = (\text{threshold}_{\text{day1}} - \text{threshold}_{\text{day2}}) / \text{threshold}_{\text{day1}} \times 100$$

The threshold % change was not significantly different from zero in the short interval group, indicating that VPL of orientation A was interfered with by the new training of orientation B (one sample 2-tailed t-test, $t(11) = -1.200$, $p = 0.255$, Figure 3).

In contrast, the threshold % change was significantly different from zero in the long interval group, showing that there was no interference of orientation A by the new training of orientation B (one sample 2-tailed t-test, $t(11) = 5.046$, $p < 0.001$). We also found a significant difference in the threshold % change between two groups (2-tailed t-test, $t(22) = -3.135$, $p = 0.005$). The results indicate that VPL is fragile against interference immediately after training but becomes stable by 3.5 hours after the training.

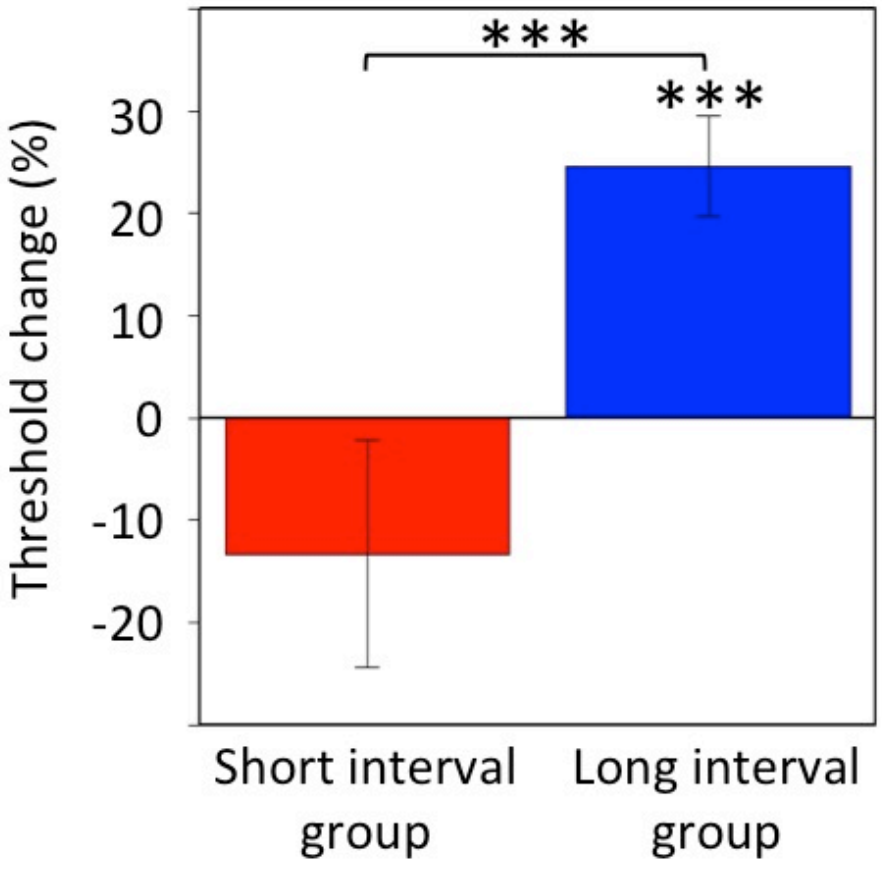

Figure 3. The performance change between day 1 and 2.

The threshold % change across day 1 and 2 for the short interval group (red) and long interval group (blue). Error bars are SEM (n=12). *** $p \leq 0.005$

2.2.3 Discussion

The current result shows that VPL is unstable immediately after training but becomes stabilized by 3.5 hours after training. It is consistent with previous findings that support wake-dependent stabilization in VPL (Seitz et al., 2005; Yotsumoto et al., 2009a). Building on this behavioral result, we can examine if the E/I ratio in the early visual cortex is changed in association with the changes in stability of VPL.

2.3 E/I ratio change is associated with wake-dependent stabilization

2.3.1 Methods

2.3.1.1 Subjects

Twelve healthy subjects (18 to 34 years old) with no use of medication participated in the experiment. All subjects had normal or corrected-to-normal vision. They kept regular wake and sleep pattern during experimental days. All subjects were informed of the purpose and the procedures of the experiment and gave written informed consent, which was approved by the Institutional Review Board of Brown University where the experiment was conducted.

2.3.1.2 Experimental design

The purpose of this experiment was to investigate if the stability of VPL is associated with changes in the E/I ratio in the early visual cortex. The behavioral result indicated that VPL is fragile immediately after training but becomes stable by 3.5 hours

after training. Thus, we measured the concentration of excitatory and inhibitory neurotransmitters in the early visual cortex (glutamate and GABA, respectively) before training (pre-training), shortly after training (post-training 1), and 3.5 hours after training (post-training 2). Then we calculated the E/I ratio by dividing the concentration of glutamate by that of GABA per session.

This experiment consisted of two consecutive days and only one orientation (orientation A) was used (Figure 4). On the first day, subjects were given a brief test session of one block for initial threshold measurement. Then a training session consisting of 8 blocks was provided. In order to track how the E/I ratio changes after training, we had MRS scans before, 30 minutes after and 3.5 hours after the training session. During the MRS scan, subjects performed a fixation task, in which central dot only was presented. Subjects were asked to detect a color change of the central dot by pressing a button. On the second day, the same test session of one block was conducted.

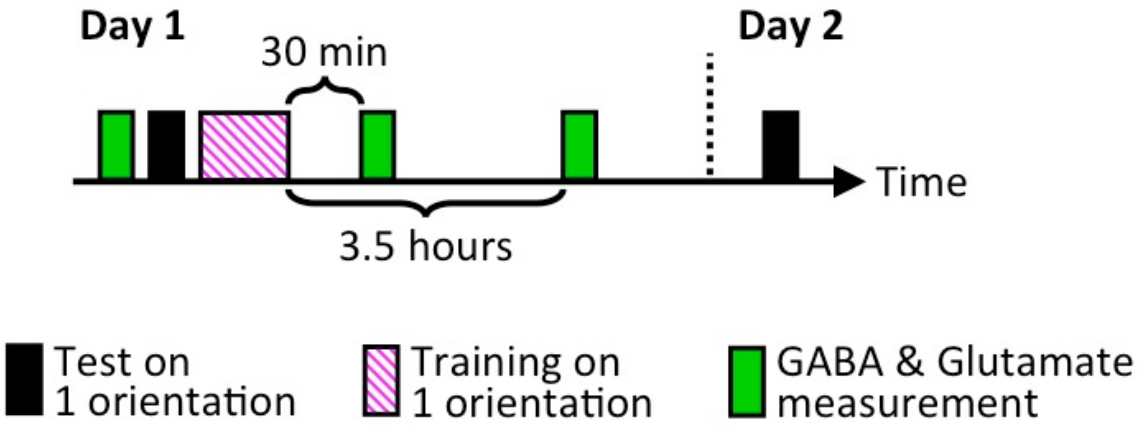

Figure 4. Experimental procedure.

2.3.1.3 Behavioral test and training sessions

The procedure of the behavioral test and training sessions was identical with that used in Chapter 2.2.1.6.

2.3.1.4 Pre-training, post-training 1, and post-training 2 sessions

Three MRS sessions were conducted in one day with the identical procedures. First, we obtained anatomical T1-weighted images. Second, based on the anatomical pictures, we positioned a voxel ($2 \times 2 \times 2cm^3$) manually along the calcarine sulcus so that the voxel covers the primary visual cortex. In the post-training 1 and post-training 2 sessions, the voxel was carefully placed on the same position as in the pre-training session. Third, an automatic shimming was performed by a vendor-provided automated shim tool. Then we manually performed a shimming to obtain the optimal shim value. This shim value was defined by a full width at half maximum of a water peak. The mean (± s.e.m) shim value across three sessions was 15.145 ± 0.147 Hz. These three steps took approximately 20-30 minutes. Finally, we measured the concentration of GABA and glutamate from the voxel. GABA and glutamate scans took 774 and 384 sec, respectively.

During GABA and glutamate scans, subjects performed a fixation task, in which they were asked to fixate their eyes at the center of the screen and report the color change of the center dot by pressing a button in a key pad. A fixation dot was placed on a gray disk and the color of the dot changed from white ([R, G, B] = [255, 255, 255]) to faint pick ([R, G, B] = [255, 255 − x, 255 − x]) in an unpredictable way and returned to white 1.5 sec later. Initially, the color change x was set to 40 and controlled by 2-down 1-up

staircase rule. If subjects pressed the button within 1.5 sec when the color of the dot changed, this response was regarded as hit. However, if subjects did not press the button within 1.5 sec when the color of the dot changed, it was regarded as miss.

2.3.1.5 MRI data acquisition

Subjects were scanned inside a 3T MR scanner (Simens Trio/Prisma) with a 32-channel head coil at Brown University MRI Research Facility. For the anatomical reconstruction, high-resolution T1-weighted MR images were acquired using a multi-echo magnetization-prepared rapid gradient echo (MEMPRAGE; 256 slices, voxel size = $1 \times 1 \times 1$ mm^3, TR = 2530 ms, TE = 1.64 ms, flip angle = 7.0 degree, TI = 1100 ms, FoV = 256 mm, bandwidth = 651 Hz/pixel).

The GABA data were obtained using a MEGA-PRESS sequence (TR = 1500 ms, TE = 68, number of average = 256, scan time = 774 sec) with double-banded pulses. Double-banded pulses were utilized to suppress water signal and edit the c-CH2 resonance of GABA at 3ppm. We subtracted the signals of alternate scans with the selective double-banded pulse applied at 4.7 and 7.5 ppm ('Edit Off) from those with the selective double-banded pulse applied at 1.9 and 4.7 ppm ('Edit On') and took it as the final spectra. The glutamate data were obtained by the PRESS sequence (TR = 3000 ms, TE = 30 ms, number of average = 128, scan time = 384 sec). In both GABA and glutamate sequences, a variable pulse power and optimized relaxation delays (VAPOR) technique was used for effective water suppression.

2.3.1.6 MRS data analysis

LC-model technique was used in all MRS data analysis. The underlying assumption of LC-model is that the obtained spectrum can be fitted in the frequency domain using a linear combination of basis functions. The Cramer-Rao Lower bounds indicate the reliability of quantification of GABA and glutamate. The mean (± s.e.m) Cramer-Rao lower bounds for GABA across participants was 6.441 ± 0.155 and that for glutamate was 4.742 ± 0.063, respectively. We normalized the amount of GABA and glutamate by using the amount of creatin, which is a standard reference resonance (Provencher, 2001). Then we took the ratio of normalized amounts of glutamate to GABA as the E/I ratio per session. An E/I ratio at the pre-training session was set to baseline individually. Then we calculated the E/I ratio change at each MRS session by using the equation:

$$E/I_{change}(t) = \left(\frac{Glu(t)/GABA(t)}{Glu(1)/GABA(1)} - 1\right) \times 100$$

Here, GABA(t) and Glu(t) represent the normalized concentrations of GABA and glutamate, respectively, at a certain MRS session t (1 = pre-training, 2 = post-training 1, 3 = post-training 2).

2.3.2 Results

To test if E/I ratio in the early visual cortex changes across three sessions, we calculated the E/I ratio changes at each session. The E/I ratio change was significantly greater than zero at post-training 1 session, indicating that the E/I ratio increased shortly

after training compared to before training (one sample 2-tailed t-test, $t(11) = 3.064$, $p = 0.011$, Figure 5). However, the E/I ratio change was not significantly different from zero at post-training 2 session, suggesting that the E/I ratio at 3.5 hours after training was not different from that before training (one sample 2-tailed t-test, $t(11) = 1.117$, $p = 0.288$). Furthermore, we found a significant quadratic trend in E/I ratio changes across three sessions ($F_{1,2} = 5.435$, $p = 0.04$). The results indicate that the E/I ratio increased shortly after training but returned close to the baseline 3.5 hours after training.

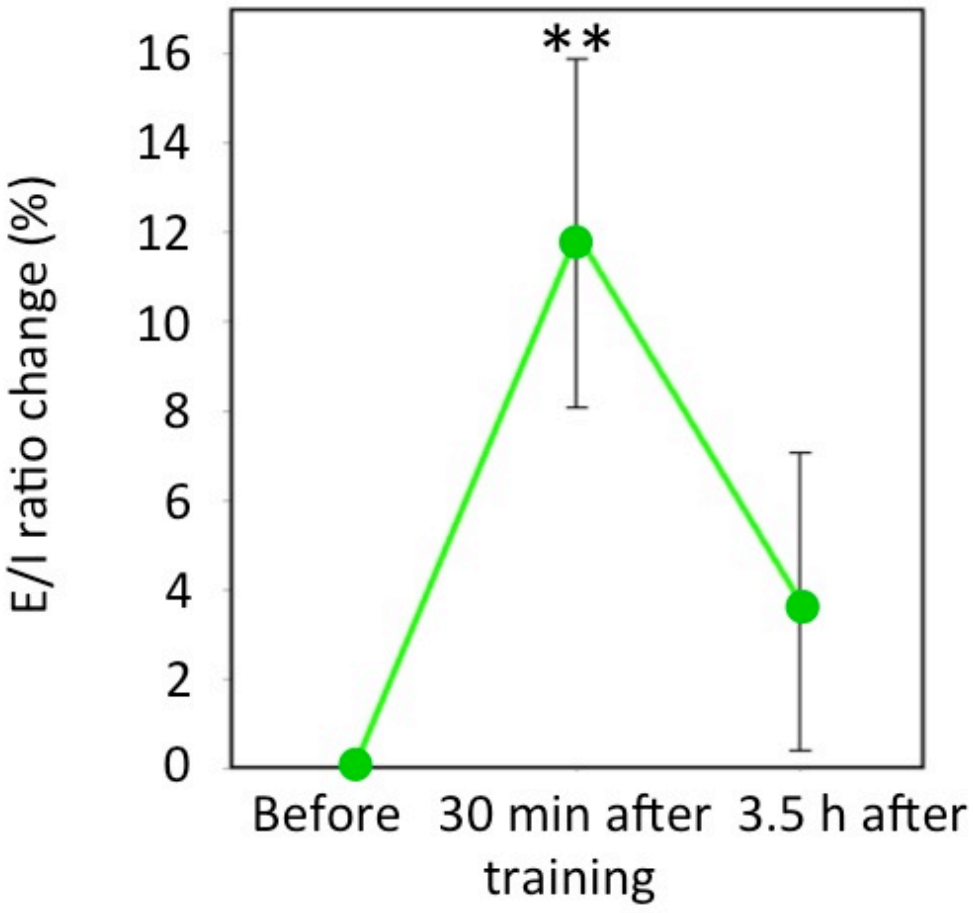

Figure 5. E/I ratio changes before, 30 minutes after and 3.5 hours after training. Error bars are SEM (n=12). ** p = 0.01

2.3.3 Discussion

The current results indicate that the E/I ratio in the early visual cortex increases shortly after training but decreases 3.5 hours after training. Interestingly, the time interval where the E/I ratio increases matched the time interval where VPL is interfered with by the following competing task. It suggests that the underlying neural mechanism of wake-dependent stabilization is associated with the E/I ratio changes in the early visual cortex. More specifically, the results suggest that the E/I ratio in the early visual cortex is high when VPL is unstable, whereas the E/I ratio is low when VPL is stable.

Interestingly, the current result fits to the framework of developmental studies in which the onset and offset of the visual critical period is determined by the E/I ratio in the visual circuit (Bavelier et al., 2010; Hensch, 2005; Morishita & Hensch, 2008). Although the underlying neural mechanisms may not be exactly the same, we can infer that the degree of plasticity of the visual system may be governed by a general process of E/I ratio changes across the critical period and adulthood.

3. Chapter 3: Sleep-dependent enhancement of VPL

3.1 Introduction

The current study under Chapter 3 aims to investigate which oscillatory activity plays a role in the consolidation of VPL, specifically within the first cycle of NREM sleep. To address this question, we trained subjects to perform a TDT in one specific quadrant of the visual field, a paradigm that is well-known to induce location-specific learning (Karni & Sagi, 1993; Yotsumoto et al., 2009b; Yotsumoto, Watanabe & Sasaki, 2008). The location specificity of the task allows us to examine activity in the trained region of early visual cortex, as well as untrained region of early visual cortex (see Chapter 3.2.6 for details). After this training, subjects slept in the lab and we recorded brain activity during sleep using magnetoencephalography (MEG) and polysomnography (PSG). Then we examined which neuronal activity among delta (0.5-4 Hz), slow sigma (11.5-12.5 Hz), and fast sigma (13.5-14.5 Hz) bands is associated with sleep-dependent enhancement in VPL. The delta activity corresponds to the frequency of slow-waves, and each sigma to slow and fast sleep spindles.

If neuronal activity in the sigma or delta bands is involved in the consolidation of TDT during NREM sleep, changes in those activities should fit the following three criteria. First, due to the location specificity of TDT learning, the power increase in the involved frequency band should be higher in the trained region compared to the untrained region. Second, due to the consolidation process, the power of the involved frequency band within the trained region of early visual areas should be higher during post-training sleep compared to pre-training sleep. Third, the difference in the oscillation power

increase between trained and untrained regions of early visual areas should be positively correlated with performance improvements.

3.2 Methods

3.2.1 Subjects

Fifteen healthy subjects (9 females and 6 males, mean age 22.53 ± 2.95) with no sleep disorders, abnormal sleep habits, or use of medication participated in the experiment. All subjects had normal or corrected-to-normal vision and refrained from caffeinated drinks and alcohol for a period of 24 hours before the experiment. Subjects were not allowed to take daytime naps on the day of the experiment. All subjects were informed of the purpose and the procedures of the experiment and gave written informed consent, which was approved by the Institutional Review Board of Massachusetts General Hospital, where the experiment was conducted.

3.2.2 Experimental design

The experiment consisted of three non-consecutive nightly sessions for MEG recording and one additional daytime session for fMRI recording (Figure 6). The first night served as an adaptation session to mitigate the "first night effect" (FNE) (Tamaki et al., 2005). FNE refers to the alteration of sleep structure that occurs when sleeping in a new environment. The second and third nights of sleep were used as the pre-training and the post-training sleeps, respectively.

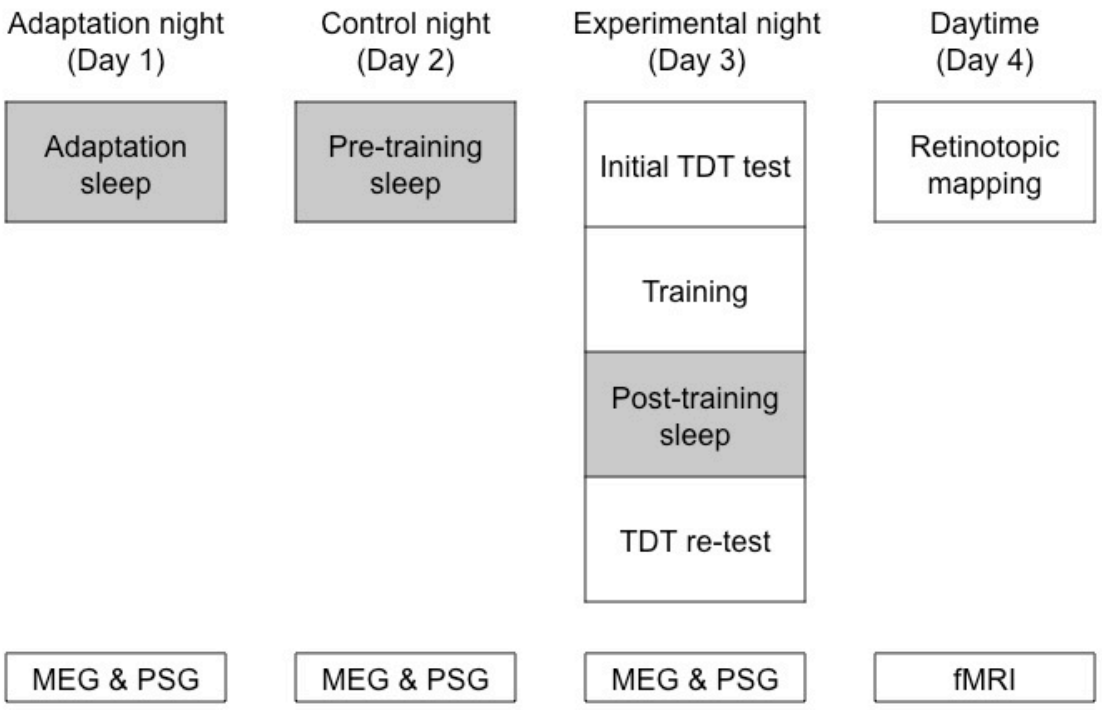

Figure 6. Experimental procedure.

There was an interval of 3-8 days between the pre- and post-training sleep sessions, during which subjects were required to maintain their regular wake-sleep pattern. The subjects' daily sleep quality and wake-sleep rhythms were monitored in self-reported sleep logs from 3 days before the experiment until the last experimental session. No subjects were excluded based on their sleep logs, since no irregularity in wake-sleep cycle was found.

In all sleep sessions, subjects slept inside a magnetically shielded room each night lying on a non-magnetic bed with their heads positioned inside the helmet-shaped tip of the dewar containing the MEG sensor array. They were allowed to sleep at their regular sleep onset time. MEG and PSG were recorded and monitored simultaneously

during sleep. Subjects were awakened when they began showing traces of the first REM sleep stage, which typically occurs 60-90 minutes after sleep onset. Waking the subjects after the first NREM sleep cycle precludes REM sleep and the following sleep cycles from exerting any possible effects on VPL. After the sleep session was over, the subjects could catch up on their sleep at home so that they would not be deprived of sleep (but see below for the timing of re-test on the third night).

On the third night, subjects conducted TDT (see below for details) before and after sleep. The initial TDT test and training of TDT were conducted five hours before sleep with no time interval between them. It is important to note that we had separated the initial TDT test, which served as a pre-training test with fewer trials, from intensive training, which involved a larger number of trials, so that the initial test would not be obscured by any possible fatigue effect (Censor, Karni & Sagi, 2006; Censor & Sagi, 2008; Mednick, Arman & Boynton, 2005; Mednick et al., 2002). The re-test was administered 30 minutes after sleep termination on the third night, before the subjects would catch up with their sleep. Thus, the re-test was conducted before any REM sleep and following sleep cycles appeared. For each subject, one specific visual field quadrant was assigned as the trained quadrant, either upper left or upper right, randomly. In addition, we measured subjects' sleepiness during the initial and re-tests by using the Stanford Sleepiness Scale (SSS) (Hoddes et al., 1973).

On the fourth day, MRI scans were conducted to obtain anatomical brain images for visualization and MEG source modeling, as well as fMRI data for retinotopic mapping to determine the boundaries between the early visual areas, including the V1,

V2, and V3. This method was consistent with previous researches (Engel et al., 1994; Fize et al., 2003; Sereno et al., 1995; Shibata et al., 2011; Yotsumoto et al., 2009b).

3.2.3 Texture discrimination task (TDT)

TDT was used for the behavioral training session that took place on the third night (Figure 7). The task was conducted in a dimly lit room. Subjects' heads were restrained in a chin rest and visual stimuli were displayed on the computer screen at a viewing distance of 57 cm. Each trial began with the presentation of a fixation point at the center of the screen (1000 ms). Then the TDT stimulus was briefly presented (13 ms), followed by a blank screen of varying duration, and finally, a mask stimulus (100 ms). The blank interval between the TDT and mask stimuli is referred to as the stimulus-to-mask onset asynchrony (SOA). When the mask stimulus is presented, new information processing in the retina overrides what remains of the TDT stimulus. Therefore, the difficulty of the task increases with decreasing SOAs. The size of the TDT display was 19º and contained a 19 × 19 array of horizontal background bars. Each bar was jittered by 0.2º. Each TDT stimulus had two components: at the center of the display, either a letter 'L' or 'T' was presented, and within the trained quadrant at a 5-9º eccentricity, three diagonal bars were presented. The diagonal bars formed either a horizontal or vertical array on the background of horizontal bars. After each trial, subjects used a button box to report whether the central letter was 'L' or 'T', and whether the three diagonal bars were aligned 'horizontally' or 'vertically'. The letter task was designed to control subjects' fixation. Mask stimuli were composed of randomly rotated v-shaped patterns. After the

subject's response, a feedback sound was delivered to indicate whether the central letter task was correct or incorrect. No feedback was given for responses on the diagonal bar task.

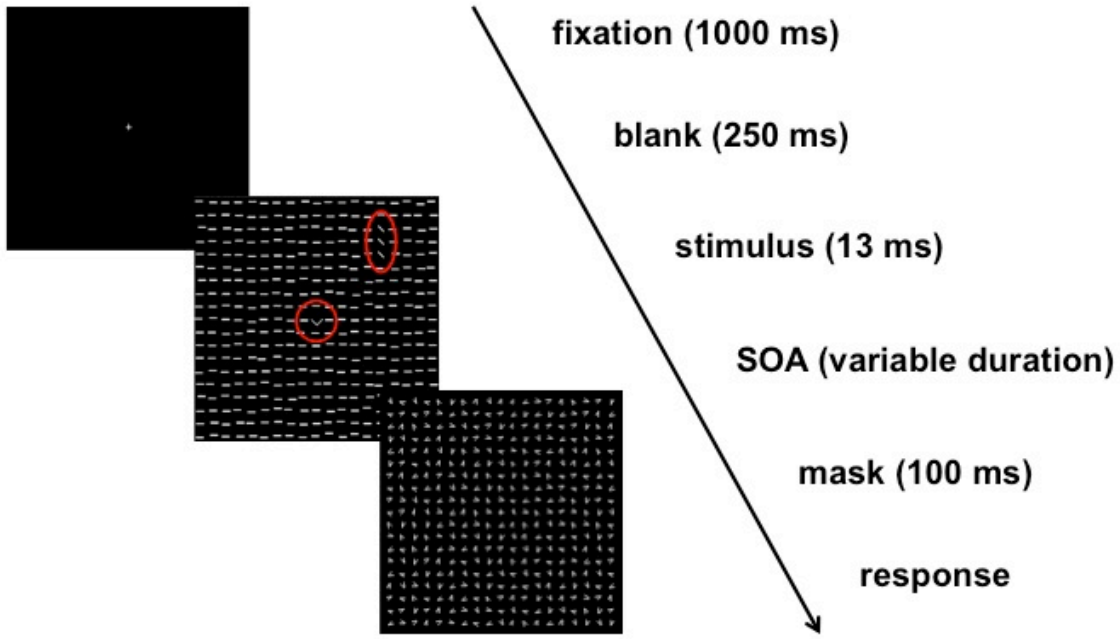

Figure 7. Texture discrimination task.

In the initial test and re-test, there were seven SOAs (400, 300, 200, 160, 130, 100, 80 ms), each presented in a block of 20 trials. The difficulty of the task thus increased from the beginning to the end of the task. After the initial test, subjects participated in an intense training session. The training session was composed of 1,620 trials with 13 SOAs (400, 300, 230, 200, 180, 170, 160, 150, 130, 120, 110, 90, 80 ms). The first 2 easiest SOAs were presented in the first 2 blocks, while the remaining 11 SOAs were distributed over 7 blocks. Each block consisted of 20 trials. SOA decreased sequentially. The training session took approximately 90 minutes.

3.2.4 MEG and PSG acquisition

MEG signals created by spontaneous brain oscillations were collected with a 306-channel Neuromag Vectorview system (Elekta Neuromag, Helsinki, Finland), which has a magnetometer and two planar gradiometers at 102 sites. Along with MEG, PSG was recorded to score the sleep stage. PSG included electroencephalogram (EEG), electrooculogram (EOG), electromyogram (EMG), and electrocardiogram (ECG). EEG was collected from four sites (C3, C4, O1, O2) referenced to the nasion. For EOG recording, electrodes were attached both above and below the left eye and at the outer canthi of the two eyes. EMG and ECG were recorded from the mentum and the chest, respectively. To co-register the anatomical MRI and the MEG data, four head position indicators (HPI) were attached on the subject's scalp. The initial head position was measured at the beginning of the MEG recording and tracked during the entirety of the sleep session (Uutela, Taulu & Hamalainen, 2001).

Subjects were asked to lie down in the bed with their head positioned inside the MEG dewar. Five minutes of data from the room void of a subject were acquired either before or after the MEG recording to estimate the noise covariance matrix for MEG source analysis. The sampling rate for MEG and EEG was 601Hz and the electrode impedance was maintained at smaller than 15kΩ.

3.2.5 MR image acquisition and analysis

Subjects were scanned in a 3-Tesla MRI scanner (Trio, Siemens). For the anatomical reconstruction, high-resolution T1-weighted MR images (MPRAGE; TR =

2.53 sec, TE = 3.28 ms, flip angle = 7°, TI = 1100 ms, 256 slices, voxel size: 1.3 × 1.3 × 1.0 mm^3) were acquired. For retinotopic mapping, functional MR images were acquired using gradient echo EPI sequences (TR = 2 sec, TE = 30 ms, flip angle = 90°, voxel size: 3 × 3 × 3.5 mm^3). Thirty-three contiguous slices oriented parallel to the AC-PC plane were acquired to cover the whole brain.

T2 functional images were corrected for motion (Cox & Jesmanowicz, 1999), smoothed with a Gaussian kernel of 5.0 mm (FWHM), and normalized individually across scans. These functional data were co-registered to the individual T1-weighted image (Dale, Fischl & Sereno, 1999; Fischl, Sereno & Dale, 1999) and the average signal intensity maps were calculated in each condition for each subject. To conduct voxel-by-voxel statistical tests, we computed contrasts based on a univariate general linear model. We projected significance levels onto the flattened cortex map individually (Dale, Fischl & Sereno, 1999; Fischl, Sereno & Dale, 1999) and localized ROIs (see below) based on these maps.

3.2.6 Retinotopic mapping and regions of interest (ROIs)

To localize the regions of interest (ROI), we used an fMRI retinotopic mapping technique for each subject. It is important to note that our ROIs were determined functionally, not anatomically. While subjects were scanned in the MRI scanner, a flickering checkerboard pattern was presented at vertical and horizontal meridians in a block design (Choi et al., 2012; Engel et al., 1994; Fize et al., 2003; Sereno et al., 1995; Shibata et al., 2012; Shibata et al., 2011; Yotsumoto et al., 2009b; Yotsumoto, Watanabe

& Sasaki, 2008). Based on the blood-oxygen-level-dependent (BOLD) signal contrast between these two meridians, the four visual quadrants of V1, V2, and V3 were localized for every subject (Engel et al., 1994; Fize et al., 2003; Sereno et al., 1995; Shibata et al., 2011; Yotsumoto et al., 2009b). Additionally, annulus stimuli were used to localize the visual field of 5°- 9° eccentricity within each quadrant (Yotsumoto et al., 2009b; Yotsumoto, Watanabe & Sasaki, 2008). This 5°- 9° eccentricity corresponds to the size of the trained visual field quadrant. Through this analysis, four sub-areas of V1, V2, and V3, which correspond to the visual field representations of upper left, upper right, lower left and lower right within 5°- 9° eccentricity, were acquired. Among the four sub-areas, one ROI corresponding to the subject's trained visual quadrant was labeled as the trained region, whereas the other three ROIs corresponding to the three untrained visual quadrants were combined into one ROI and labeled as the untrained region. We also combined the trained and untrained regions as a reference to normalize the activation of the separate trained and untrained regions (see below). Therefore, there were 9 ROIs in total: the trained, the untrained, and the reference regions in V1, V2, and V3.

3.2.7 PSG and MEG data analysis

The sleep stages from PSG data were scored as wake, stage 1, stage 2, SWS or REM sleep for every 30 second epoch in accordance with the American Academy of Sleep Medicine (AASM) scoring manual (Iber, 2007). In the subsequent analysis, only the epochs scored as NREM sleep (stage 2 and SWS) were used.

We analyzed MEG data recorded from 306 channels. To estimate MEG power sources in the individual cortical surface using anatomical MRI, we used recently developed technique, which combines a cortically constrained minimum norm estimate (MNE) and spectral analysis utilizing Morlet wavelets (Ahveninen et al., 2007; Lin et al., 2004). To compensate for head motion and to reduce noise, the MEG data were processed with the maxfilter software (Elekta-Neuromag, Helsinki, Finland). Then, the data were band-pass filtered between 0.1 Hz and 50 Hz. The continuous Morlet wavelet transform was applied to the filtered data and the spectral power was calculated for every 30 second epoch per each of the chosen frequency bands (Ahveninen et al., 2007; Lin et al., 2004). The frequency bands that we analyzed were delta (0.5-4 Hz), slow sigma (11.5-12.5 Hz) and fast sigma (13.5-14.5 Hz), as mentioned above.

In order to calculate a location-specific power for each ROI, we averaged spectral power across every voxel within each ROI per epoch. Then we averaged each ROI's spectral power across every epoch within stage 2 sleep and SWS, respectively. To normalize the mean power of trained and untrained ROIs for each sleep stage between the pre- and post-training sleep sessions, we divided it by the mean power of reference ROI of the corresponding night session's sleep stages. Then we computed the power change index for trained and untrained ROIs by subtracting the normalized mean power of each ROI of pre-training sleep from the normalized mean power of the same ROI of post-training sleep:

Power change index = $p(i, post) / p(3, post) – p(i, pre)/p(3, pre)$

where p(i, post/pre) represents mean power within region i (1 = trained, 2 = untrained, 3 = reference) computed from either post/pre- training. The power change index was calculated for trained and untrained V1, V2, and V3 during stage 2 sleep and SWS, separately. Since we were interested in delta, slow sigma, and fast sigma bands, the power change index was obtained for these three frequency bands.

3.3 Results

3.3.1 Sleep structure for pre- and post-training sleep sessions

To confirm that the first night effect did not confound the sleep structure between the pre- and post-training sleep sessions, a paired t-test was conducted for each variable. As shown in Table 1, there were no significant differences in any of these sleep variables between the pre- and post-training sleep sessions. Thus, we confirmed that the first night effect did not confound the sleep structure in the pre- and post-training sleep sessions.

Table 1. Sleep variables

	Pre-training sleep		Post-training sleep		*P* value
	mean	s.e.m.	mean	s.e.m.	
Total sleep time (min)	80.1	4.16	77	2.53	0.47
Wake (min)	10.8	2.96	6.88	1.69	0.12
Stage 1 (min)	19.3	3.53	16	3.78	0.44
Stage 2 (min)	22.5	2.69	22.5	2.83	0.99
SWS (min)	37.1	4.68	36.8	5.17	0.94
REM sleep (min)	1.17	0.81	1.66	0.92	0.71
Waking after sleep onset (min)	3.92	1.62	3.04	1.48	0.63
Wake (%)	11.4	3.2	7.79	1.78	0.19
Stage 1 (%)	21	3.92	18.5	4.21	0.59
Stage 2 (%)	24.8	2.93	26.7	3.01	0.61
SWS (%)	41.4	5.3	45	6.35	0.55
REM sleep (%)	1.19	0.74	1.95	1.05	0.58
Waking after sleep onset (%)	4.18	1.81	3.41	1.59	0.70
Sleep efficiency (%)	88.7	3.22	92.2	1.78	0.22

Table 1. Sleep variables.

Sleep efficiency was measured as the ratio of total sleep time to the amount of time spent in bed. No significant difference was found between pre-training and post-training sleep for any of the sleep variables (paired t-test).

3.3.2 Behavioral results and sleepiness

We calculated the percentage of correct responses for the diagonal bar task for each SOA. A logistic function was fitted to each individually measured psychometric data to determine the threshold SOA corresponding to 80% correct performance. This was done for both the initial test and re-test using the psignifit toolbox (ver. 2.5.6) for Matlab (http://bootstrap-software.org/psignifit/). This software package implements the maximum-likelihood method described by Wichmann and Hill (2001). To test whether learning occurred in the trained quadrant, the 80% threshold SOAs in the initial test and re-test were compared (Figure 8). There was a significant difference between the initial and re-tests, indicating that learning occurred after sleep (2-tailed paired t-test, $t(14) = 3.571$, $p = 0.003$). The result of the training session is shown in Figure 9.

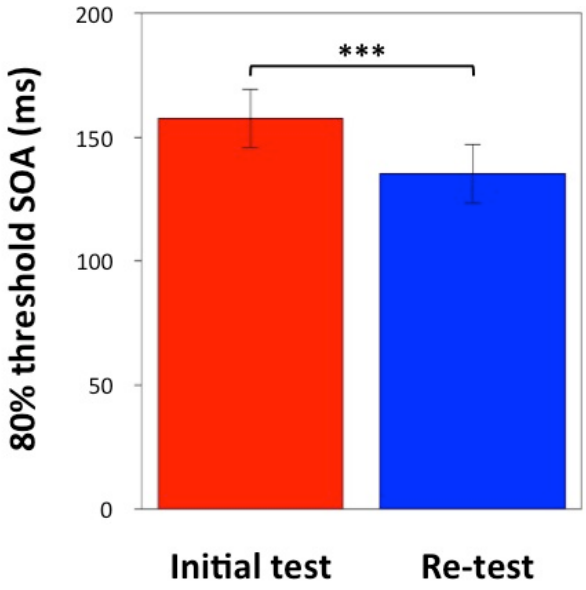

Figure 8. The performance improvement after sleep.

The 80% threshold SOA for the initial (red) and re-test (blue). Error bars are SEM (n=15). *** p = 0.003

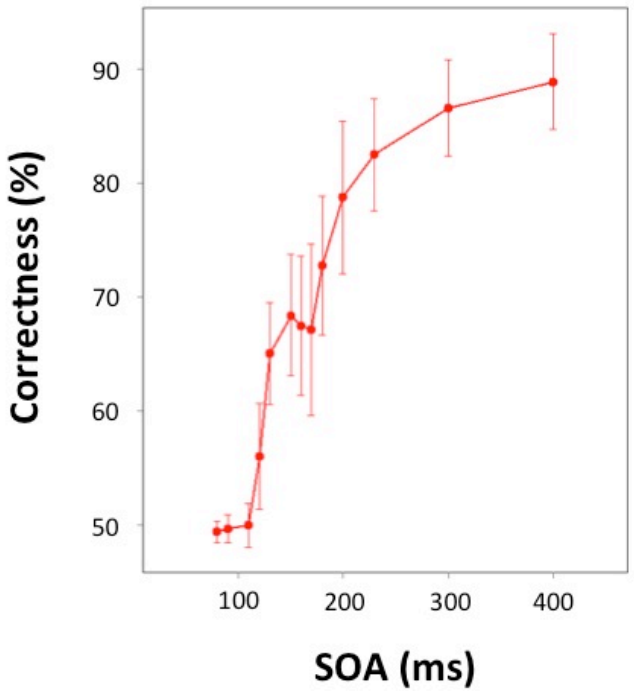

Figure 9. Line plot representing the percentage of correctness (%) as a function of SOA (ms) in the training session. Error bars are SEM (n=15).

The results of the SSS at the initial test and re-test did not indicate a significant difference. The average (± SE) score of the SSS was 2.6 ± 0.36 for the initial test and 2.9 ± 0.27 for the re-test (2-tailed paired t-test, $t(14) = -0.576$, $p = 0.57$). The higher the score of the SSS is, the sleepier the subject is (Hoddes et al., 1973). The score of the SSS suggests that the subjects were sleepier at the re-test than at the initial test, although it was not statistically significant. In contrast, the performance of TDT at the re-test was significantly better than at the initial test. Thus, the SSS results suggest that the performance improvement was not caused by higher alertness at the re-test.

3.3.3. MEG results

The power change index of each frequency band (delta, slow sigma, and fast sigma) was calculated for each of the trained and untrained regions of early visual areas (V1, V2, and V3) and sleep stages (stage 2, and SWS). We used a four-factor repeated measures of ANOVA to examine whether there were main effects of sleep stage (stage 2, and SWS), frequency (delta, slow sigma, and fast sigma), training (trained, and untrained) and location (V1, V2, and V3), as well as interactions between them during the first NREM sleep cycle, on a power change index, as the dependent measure. In this model, sleep stage, frequency, training, and location were fixed factors, and subject was a random factor. We found significant interactions in the sleep stage × frequency ($F_{2,486} = 3.179$, $p = 0.042$) and sleep stage × frequency × training ($F_{2,486} = 7.491$, $p = 0.001$), while none of significant main effects of sleep stage, frequency, training and location was found.

Since these two- and three-factor interactions were significant, we applied a two-factor repeated measures of ANOVA (factors: frequency and training) to the data for each sleep stage (stage2 and SWS), separately. During sleep stage 2 (Figure 10A), we found a significant main effect of frequency ($F_{2,264} = 3.360$, $p = 0.036$), and training ($F_{1,264} = 4.387$, $p = 0.037$). In addition, there was a significant interaction between training and frequency on the power change index ($F_{2,264} = 7.531$, $p = 0.001$). Given the interaction between the training and frequency, Tukey's post-hoc test, which corrects for an experiment-wise error rate, revealed that the power change index of slow sigma activity was significantly greater in the trained region compared to the untrained region

(p = 0.007), whereas no significant difference was found in the power change index of delta and fast sigma activity between the trained and untrained regions.

In contrast, no significant main effect was observed during SWS (Figure 10B), although there was only a marginal interaction between training and frequency ($F_{2,246}$ = 2.629, p = 0.074). This suggests that none of three frequencies' activity changed meaningfully between the trained and untrained regions during SWS.

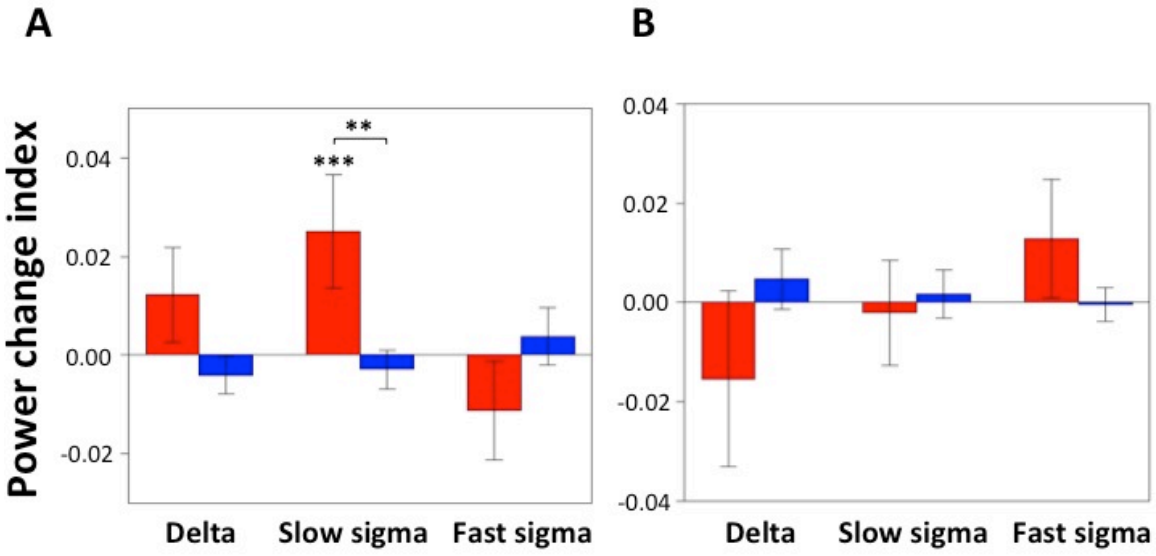

Figure 10. Mean (± 1 SEM) change index for the trained (red) and untrained (blue) regions in early visual areas during stage 2 (A) and during SWS (B). ** p < 0.01, *** p < 0.005

Among three frequency bands during sleep stage 2, only the slow sigma activity satisfied the first criterion: the power increase should be greater in the trained region of early visual areas than in the untrained region. Therefore, we further tested whether slow sigma activity satisfies the second criterion, which is that the power of the trained region should be higher in the post- than in the pre-training sleep. The following test showed

that the normalized mean power of slow sigma activity within the trained region during sleep stage 2 was significantly greater in the post- than in the pre-training sleep (2-tailed paired t-test, $t(44) = 3.125$, $p = 0.003$). This indicates that the slow sigma activity increased after training specifically within the trained region of early visual areas.

Finally, we tested whether the changes in the slow sigma band were correlated with the performance improvement after sleep. Interestingly, we found a significant correlation between the performance improvement and the difference of slow sigma power change indices between the trained and untrained regions during sleep stage 2 (2-tailed Pearson's correlation, $r = 0.6934$, $p = 0.004$, $n = 15$, Figure 11). The Grubbs' test for outliers in the performance improvement and in the difference of slow sigma power change indices ($p = 0.608$ and $p = 0.609$, respectively) indicated that there is no outlier in the plot. This implies that the larger the discrepancy of power increases between the trained and untrained regions, the more the subject learned. In contrast, none of the difference of delta, and fast sigma's power change indices during sleep stage 2, and the difference of delta, slow, and fast sigma's power change indices during SWS, showed any correlation with performance improvement ($r = -0.183$, $p = 0.514$; $r = 0.375$, $p = 0.169$; $r = -0.274$, $p = 0.342$; $r = 0.051$, $p = 0.863$; $r = 0.185$, $p = 0.527$, respectively).

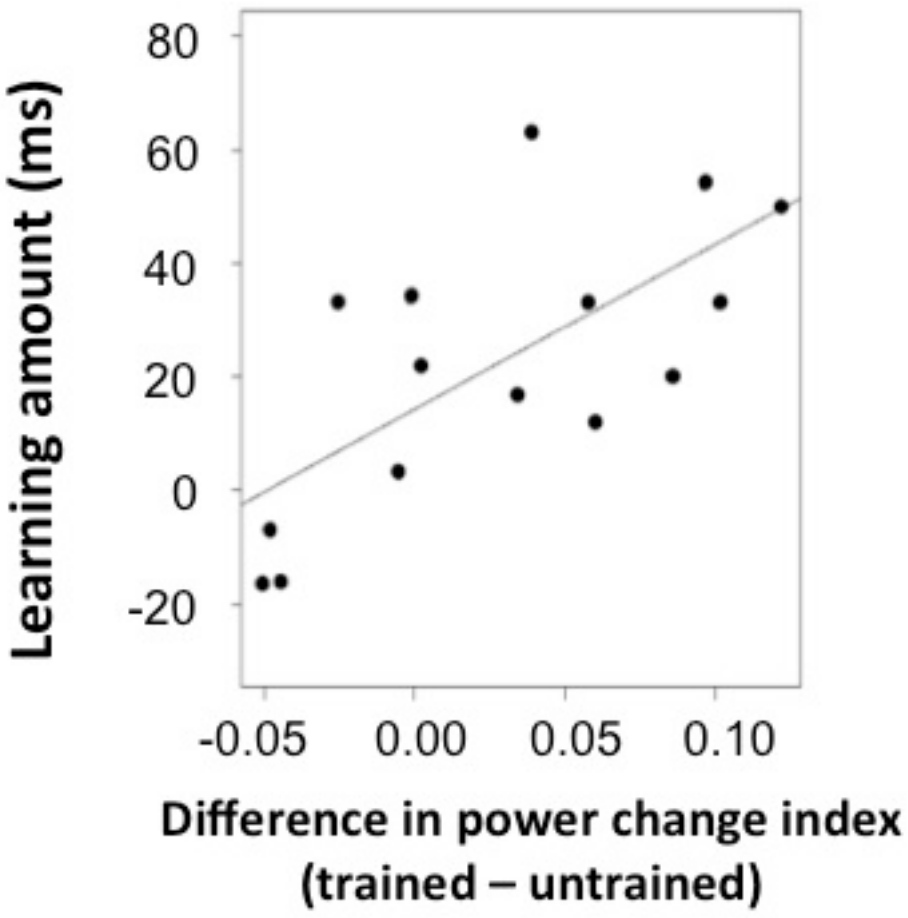

Figure 11. Scatter plot representing the correlation between threshold improvement and the difference in sigma band power indices between trained and untrained regions within early visual areas (averaged across V1, V2, V3) during sleep stage 2.

3.4 Discussion

In the present study, we took advantage of the location specificity that occurs in VPL of the TDT and investigated whether slow/fast sigma or delta band activity was involved in the consolidation of VPL during NREM sleep, using MEG, MRI and PSG in combination. As mentioned earlier, we tested whether the slow/fast sigma or delta activity satisfied three criteria: (1) greater power increase in the trained compared to the

untrained region of early visual areas, (2) greater power in the post- compared to the pre-training sleep sessions, and (3) positive correlation between performance improvement and the difference of power increase between the trained and untrained regions of early visual areas. The behavioral test indicated significant off-line learning after sleep, as has been shown previously (Gais et al., 2000; Karni & Sagi, 1993; Stickgold, James & Hobson, 2000; Stickgold et al., 2000; Yotsumoto et al., 2009b). Among the slow/fast sigma and delta activities, we found that only slow sigma activity, specifically within sleep stage 2, satisfied the criteria. On the other hand, none of slow/fast sigma and delta activity satisfied the criteria during SWS.

Our results indicate that slow sigma activity during sleep stage 2 is involved in the consolidation of TDT, at least during the first sleep cycle. It has been suggested that sleep spindles play a critical role in sleep-dependent consolidation of various kinds of learning and memory (Clemens, Fabo & Halasz, 2005, 2006; Fogel & Smith, 2006; Gais et al., 2002; Molle et al., 2009; Morin et al., 2008; Nishida & Walker, 2007; Rosanova & Ulrich, 2005; Schabus et al., 2004; Schmidt et al., 2006; Wamsley et al., 2012). Since sigma activity corresponds to sleep spindles, our results are consistent with the other studies that have suggested that sleep spindle activity is involved in consolidation (Clemens, Fabo & Halasz, 2005, 2006; Fogel & Smith, 2006; Gais et al., 2002; Molle et al., 2009; Morin et al., 2008; Nishida & Walker, 2007; Rosanova & Ulrich, 2005; Schabus et al., 2004; Schmidt et al., 2006; Wamsley et al., 2012). Increased spindle activity was found after the learning of a declarative memory task (Gais et al., 2002; Molle et al., 2009; Schabus et al., 2004; Schmidt et al., 2006), a motor procedural task (Fogel & Smith, 2006; Morin et al., 2008) and was correlated with overnight gains in verbal and motor tasks (Clemens,

Fabo & Halasz, 2005, 2006; Nishida & Walker, 2007; Schabus et al., 2004). Our finding adds to the growing body of evidence suggesting that spindle activity is involved in the consolidation of a visual task, and is associated with the overnight improvement in TDT performance.

Because spindle-associated spike trains can induce LTP in cortical synapses (Rosanova & Ulrich, 2005), it has been suggested that newly acquired memories are "replayed" during sleep via sleep spindles (Bergmann et al., 2012; Born, Rasch & Gais, 2006; Born & Wilhelm, 2012; Hasselmo, 1999; Rasch et al., 2007). The replay of memory traces during sleep has been reported in both animal and human studies. In rats and zebra finches, the bursting patterns from large numbers of neurons observed during maze tasks or song learning were reactivated during subsequent NREM sleep (Dave & Margoliash, 2000; Ji & Wilson, 2007; Margoliash, 2010; Wilson & McNaughton, 1994). In human studies, memory replay-like enhanced activity was observed in the hippocampus after learning a spatial task (Peigneux et al., 2004), in the neocortex and hippocampus after learning face-scene associations (Bergmann et al., 2012), and in the trained region of V1 during NREM sleep after learning TDT (Yotsumoto et al., 2009b). Importantly, it has been found that enhanced BOLD signals are time-locked with sleep spindles (Bergmann et al., 2012). These findings suggest that the trained visual representations used in our study were reactivated through sleep spindles during sleep stage 2, although the question of which representation the neurons were "replaying" presents an exciting avenue of future research.

There are two major models of consolidation processes during sleep: the active system consolidation model (Born, Rasch & Gais, 2006; Born & Wilhelm, 2012;

Hasselmo, 1999; Rasch et al., 2007) and the synaptic homeostasis model (Tononi & Cirelli, 2003, 2006). The results of the present study favor the active system consolidation model, since the enhanced slow sigma power we observed corresponds to slow sleep spindle activity. It implies that an active replay process occurred in the trained region of early visual areas during sleep. However, several discrepancies between this model and our results must be noted. First, significant power increases in the slow sigma band were restricted to sleep stage 2, whereas the model assumes that memory replay occurs during both sleep stage 2 and SWS (NREM sleep). Therefore, it is not clear whether this present stage 2 specific slow sigma power increase is consistent with the active system consolidation model. Second, delta band activity, corresponding to slow-waves, did not increase during either sleep stage 2 or SWS, whereas the model suggests that slow-waves also play a role in the replay and redistribution process. Slow-waves temporally group neuronal activity to depolarizing up-states not only in the neocortex, but also in various brain structures via efferent pathways (Steriade, 2006). Thus, slow-waves may provide a temporal frame globally, during which the up-states drive memory replay in neocortex in parallel with other brain regions (Born & Wilhelm, 2012). The active system consolidation model highlights this feature of slow-waves because this process is thought to transfer reactivated memory information, particularly in the declarative memory system between the temporary and long-term storages. However, this redistribution concept is yet to be confirmed in VPL. Therefore, future studies are needed to examine how the consolidation process differs between VPL and declarative memory systems.

Our results do not directly support the synaptic homeostasis model, which assumes that slow-waves are a key component of consolidation (Tononi & Cirelli, 2003, 2006), because we found no significant delta power increase. However, it is still possible that the process proposed by the synaptic homeostasis model acts in concert with replay at the neuronal level in subsequent NREM sleep cycles, which were not measured in the present study.

This study separated sleep spindle activity into slow and fast spindles based on previous findings (Anderer et al., 2001; Schabus et al., 2007; Schabus et al., 2008; Tamaki et al., 2009; Werth et al., 1997; Zeitlhofer et al., 1997; Zygierewicz et al., 1999). Slow and fast sleep spindles differ not only by frequency but also by the scalp distribution. Slow sleep spindles appear dominantly over the frontal part of the brain, whereas fast sleep spindles prevail over the centro-parietal region (Anderer et al., 2001; Schabus et al., 2007; Werth et al., 1997; Zeitlhofer et al., 1997). The present study found the involvement of the slow sigma band from the occipital region in the consolidation of VPL. Thus, the locus of slow sigma oscillations in the present study may seem inconsistent with the previous studies that reported predominance of slow spindles over the frontal region. However, it is questionable whether each type of sleep spindle serves to consolidate learning only within their known dominant loci of the brain. In the case of fast spindles, their predominant area was consistent with the region where they consolidate learning: fast sleep spindles were found to be involved in the consolidation of motor learning through the activation in motor related areas, which are located at the central region (Barakat et al., 2011; Schabus et al., 2007; Tamaki et al., 2013; Tamaki et al., 2008, 2009). On the other hand, slow spindles' dominant loci seem to be different

from the region where they consolidate VPL. This implies that roles of slow spindles in consolidation could go beyond the dominant loci depending on the task and the brain areas where the task related consolidation occurs.

One may wonder whether the present results are inconsistent with a previous study that showed a negative relationship between sleep spindles and perceptual learning (Mednick et al., 2013). We argue that these studies are not necessarily inconsistent with each other, given that there are several significant methodological differences. First, a pharmacological intervention was used to enhance sleep spindle activity during the daytime nap in the previous study (Mednick et al., 2013), whereas the present study investigated the endogenous sigma oscillations during nocturnal sleep. It is an open question whether the spindle activity caused by a pharmacological intervention during a daytime nap has the same neural origin or plays the same role in learning as endogenous spindles during the night.

Second, brain regions where the spindle activities originated from may differ between the present and previous studies (Mednick et al., 2013). Mednick et al. (2013) visually counted the number of sleep spindles observed in EEG channels C3 and C4. In contrast, we investigated the sigma power, which was source-localized in early visual areas. Indeed, Mednick et al (2013) has suggested that spindle activity observed in the central region in their study is crucially involved in hippocampal activity. In contrast, the sigma activity investigated in the current study represents activity in the early visual cortex. It has been found that activity in the early visual areas change as VPL of TDT occurs (Schwartz, Maquet & Frith, 2002; Walker et al., 2005; Yotsumoto, Watanabe & Sasaki, 2008), especially during the following sleep after the initial training (Yotsumoto

et al., 2009b). Given these differences, it would be premature to state that the previous (Mednick et al., 2013) and present studies are inconsistent in terms of the relationship between VPL and spindle activity.

One may also wonder whether the NREM effect shown in the present study reflects mere amelioration of deterioration, rather than improvements as a result of the consolidation process. The deterioration here refers to the worsening in performance compared to the previous session, due to fatigue caused by the intensive training session (Censor, Karni & Sagi, 2006; Censor & Sagi, 2008; Mednick, Arman & Boynton, 2005; Mednick et al., 2002). However, it is unlikely that the current results reflect only amelioration of deterioration for the following reasons. First, in our study, the initial TDT test was separated from training, so that the initial performance threshold would not be masked by any fatigue effects, which may occur with a large number of trials during training (Censor, Karni & Sagi, 2006; Censor & Sagi, 2008; Mednick, Arman & Boynton, 2005; Mednick et al., 2002). In addition, there were only 140 trials in the initial test of the present study. A previous study suggested that a total of 450 trials per session may not cause deterioration (Censor & Sagi, 2008). Second, in our earlier work (Yotsumoto et al., 2009b) that included careful control experiments, the performance improvement, but not deterioration, was found in TDT with a training period of 1760 trials, which was larger than the current number of trials (1620 trials) in training. Third, more importantly, we have found a significant and high correlation between performance improvement and the difference in slow sigma power change indices, indicating a tight connection between the sleeping brain and learning (Figure 11). Thus, the NREM effect in the present study is highly likely to represent a neural process involved in the consolidation of TDT.

It should be noted that an accumulating body of evidence suggests a multifaceted consolidation process of sleep in facilitating VPL (Stickgold et al., 2000). Although we restricted our study to the effect of the first sleep cycle's NREM sleep only, this does not necessarily indicate that we do not acknowledge possible roles of REM sleep (Karni et al., 1994; Mednick, Nakayama & Stickgold, 2003; Stickgold et al., 2000). The possible roles of REM sleep and later sleep cycles in facilitating VPL need to be addressed in the near future.

The present study investigated which component of NREM sleep is involved in the consolidation of TDT, as a representative task of VPL. However, the neural mechanism of VPL in general has been controversial. Perhaps, this is because the neural process involved in VPL is affected by various factors (Lu et al., 2011; Sagi, 2011; Sasaki, Nanez & Watanabe, 2010). The neural site of VPL may shift and change over the course of training. Yotsumoto et al. (2008) showed that early visual areas were significantly involved in the early phase of training. However, in the later phase of training, the activation level of early visual areas returned to the baseline. Other researchers argue that VPL reflects deployment of attention (Xiao et al., 2008; Zhang et al., 2010a; Zhang et al., 2010b) or changes in the process to read out sensory information by decision areas (Huang, Lu & Dosher, 2012; Law & Gold, 2008; Petrov, Dosher & Lu, 2006). It should be noted that in the present study, we focused on the brain activation of early visual areas during sleep, but not higher brain regions. Therefore, integrative studies are needed to fully understand the mechanisms of VPL in the near future

4. Chapter 4: Reactivation and reconsolidation processes of VPL

4.1 Introduction

Previous findings in the declarative, fear and motor memory domains indicate that memory retrieval can change the existing memory into a labile state once again, thus making it susceptible to interference from competing tasks (Chan & LaPaglia, 2013; Forcato et al., 2007; Hupbach et al., 2007; Walker et al., 2003). Inspired by this line of researches, we aimed to investigate if reactivation returns previously consolidated VPL into fragile state against interference again. Furthermore, we examined if the E/I ratio in early visual areas is associated with the reactivation. Developmental studies suggest that the start and end of a visual critical period in animals' early life are associated with significant changes in the E/I ratio in visual circuits (Bavelier et al., 2010; Hensch, 2005; Morishita & Hensch, 2008). Previous finding in Chapter 2 also suggests that the E/I ratio in the early visual cortex increases during which the visual system is plastic. Building on these studies, we tested if the E/I ratio in the early visual cortex changes in association with reactivation. In addition, we investigated if the reactivation is a general process in VPL regardless of the stimulus that is used for training and reactivation.

4.2. Reactivation makes consolidated VPL fragile again

4.2.1 Methods

4.2.1.1 Subjects

Twenty-four healthy subjects (6 males and 18 females, mean age 20.92 ± 2.59) with no use of medication participated in the experiment. All subjects had normal or corrected-to-normal vision and had no habit of playing video games. They kept regular wake and sleep pattern during experimental days. All subjects were informed of the purpose and the procedures of the experiment and gave written informed consent, which was approved by the Institutional Review Board of Brown University where the experiment was conducted.

4.2.1.2 Experimental design

To examine whether previously consolidated VPL becomes fragile immediately after reactivation but becomes stable with a passage of time, we used orientation detection task with two orientations, 10 and 70 degree. Two orientations were randomly assigned to orientation A (firstly trained orientation) and B (secondly trained orientation) across subjects. In addition, subjects were randomly assigned to either short or long interval group. In the short interval group, there was no explicit time interval between the reactivation of firstly trained orientation A and new training of orientation B, whereas in the long interval group, there was 3.5 hours interval. The purpose of having two groups

was to test if the stability of reactivated VPL changes as a function of time interval between reactivation and new learning of orientation B.

The entire behavioral experiment consisted of three consecutive days (Figure 12). On the first day, subjects were given a brief test session consisting of three blocks of orientation A. The purpose of the test session was to measure the initial threshold for orientation A per subject. The first block served as a practice and the rest following two blocks were used for threshold measurement. After the test session, subjects were provided with the training session of orientation A consisting of 16 blocks.

On the second day, the firstly trained orientation A was briefly reactivated through test session of orientation A. In the short interval group, this test session was immediately followed by another test and training sessions of orientation B. In contrast, subjects in the long interval group were given test and training sessions of orientation B 3.5 hours after the test session of orientation A. If reactivated VPL becomes fragile shortly after reactivation, interference of orientation A by the second learning of orientation B should occur in the short interval group. However, if reactivated VPL becomes stable 3.5 hours after reactivation, interference of orientation A by the second learning of orientation B should not occur in the long interval group.

On the third day, subjects were provided with test sessions of orientation A and B. By comparing the performance on orientation A between the second and the third day, we can examine if new learning of orientation B interfered with reactivated VPL of orientation A.

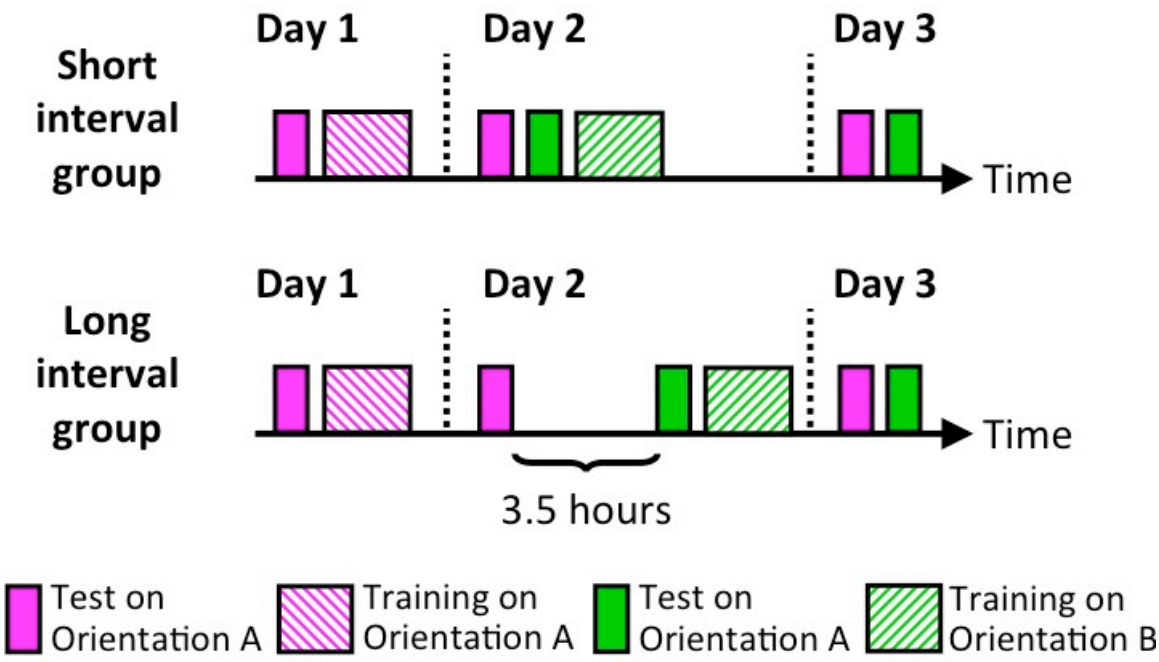

Figure 12. Experimental procedure.

4.2.1.3 Gabor stimulus

Gabor patches with one orientation (contrast = 100%, spatial frequency = 1 cycle/degree, sigma of its Gaussian filter = 2.5 degree, random spatial phase) were presented within an annulus covering 0.34 to 2.25 degree from the center of the screen. Noise pattern generated from a sinusoidal luminance distribution was superimposed on the Gabor patches and it yielded a certain signal to noise (S/N) ratio.

4.2.1.4 Orientation detection task

The task was identical with that used in the Chapter 2's behavioral experiment (Chapter 2.2.1.4).

4.2.1.5 Threshold measurement

Each subject's threshold S/N ratio in each block was determined by 2-down 1-up staircase rule. This method yields 70.7% accuracy rate. Each block started with 25% S/N ratio and terminated after 10 reversals. Each block consisted of 30-40 trials and took 1-2 minutes approximately. We took the geometric mean of the last 6 reversals as a threshold S/N ratio per each block (Xiao et al., 2008). Then, the geometric mean of the threshold S/N ratio across blocks was taken as the final threshold per subject.

4.2.1.6 Behavioral test and training sessions

In the behavioral test session, subjects were given three blocks of one orientation, which lasted roughly 4-6 minutes. The orientation was randomly chosen among 10 and 70 degree. The first block served as a practice and the rest two blocks were used to measure the threshold S/N ratio.

During the behavioral training session, subjects were provided with 16 blocks of one orientation. This behavioral training session took approximately 40 minutes.

4.2.2 Results

4.2.2.1 Learning occurs after training

Before testing whether the reactivated VPL becomes labile against interference of the secondly trained orientation B, we first examined if the firstly learned orientation A went through consolidation process between the first and the second day. Previously, it was mentioned that there are two phases in the consolidation of VPL: wake-dependent stabilization and sleep-dependent enhancement. These two processes are known to occur during the subsequent wakefulness and sleep after training. Thus, one way of examining whether the firstly learned orientation A went through consolidation is to examine if the performance on the firstly trained orientation A improved between the first and the second day.

To test this, we took the geometric mean of the threshold S/N ratio across two blocks in the test session as the final threshold S/N ratio per subject and computed how much change occurred between the first and the second day using an equation below:

$$\text{Threshold \% change}_{\text{day1 \& 2}} = (\text{threshold}_{\text{day1}} - \text{threshold}_{\text{day2}}) / \text{threshold}_{\text{day1}} \times 100$$

The threshold % change was significantly greater than zero for both short and long interval groups, indicating that performance on orientation A improved on the second day compared to the first day (one sample 2-tailed t-test, $t(11) = 6.422$, $p < 0.005$ for short interval group; one sample 2-tailed t-test, $t(11) = 9.715$, $p < 0.005$ for long interval group, Figure 13). There was no significant difference in the threshold % change between two groups (2-tailed t-test, $t(22) = -0.591$, $p = 0.56$). The results suggest that

orientation A went through consolidation process in both two groups after the initial training.

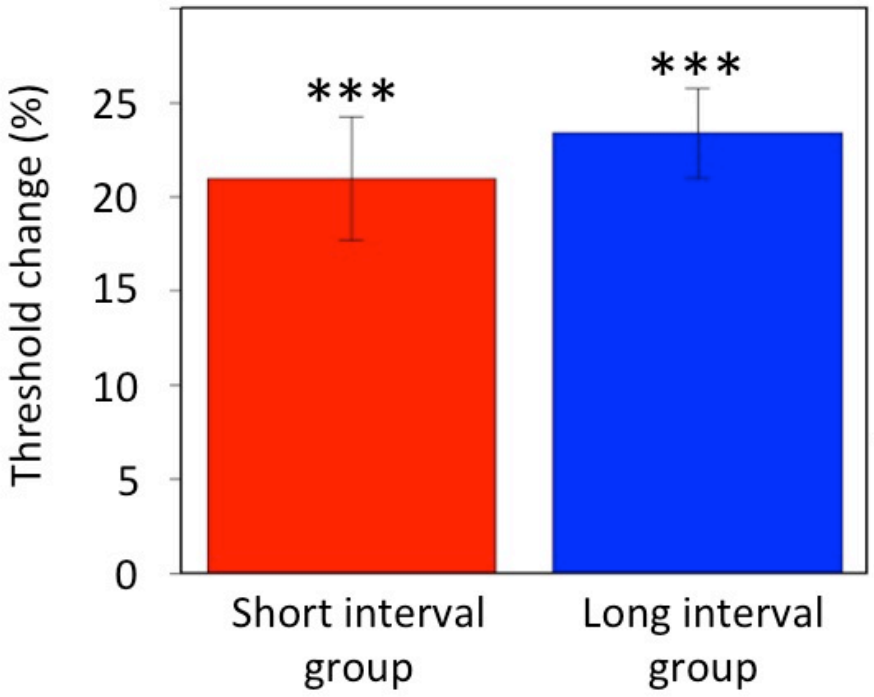

Figure 13. The performance improvement between day 1 and 2.

The threshold % change across day 1 and 2 for the short interval group (red) and long interval group (blue). Error bars are SEM (n=12). *** p < 0.005

4.2.2.2 Consolidated VPL becomes fragile against interference immediately after reactivation, but becomes stable 3.5 hours after reactivation

To test whether reactivation makes previously consolidated VPL fragile against interference, we computed the threshold % change of orientation A across the second and the third day per subject:

$$\text{Threshold \% change}_{\text{day2 \& 3}} = (\text{threshold}_{\text{day2}} - \text{threshold}_{\text{day3}}) / \text{threshold}_{\text{day2}} \times 100$$

The threshold % change was significantly lower than zero in the short interval group, indicating that the reactivated VPL was interfered with by the new training of orientation B (one sample 2-tailed t-test, $t(11) = -3.254$, $p = 0.008$, Figure 14). In contrast, the threshold % change was not significantly different from zero in the long interval group, showing that there was no interference of the reactivated VPL by the new training of orientation B (one sample 2-tailed t-test, $t(11) = 0.553$, $p = 0.592$). We also found a significant difference in the threshold % change between two groups (2-tailed t-test, $t(22) = -2.453$, $p = 0.023$). The results indicate that previously consolidated VPL becomes fragile against interference immediately after reactivation but becomes stable again 3.5 hours after the reactivation.

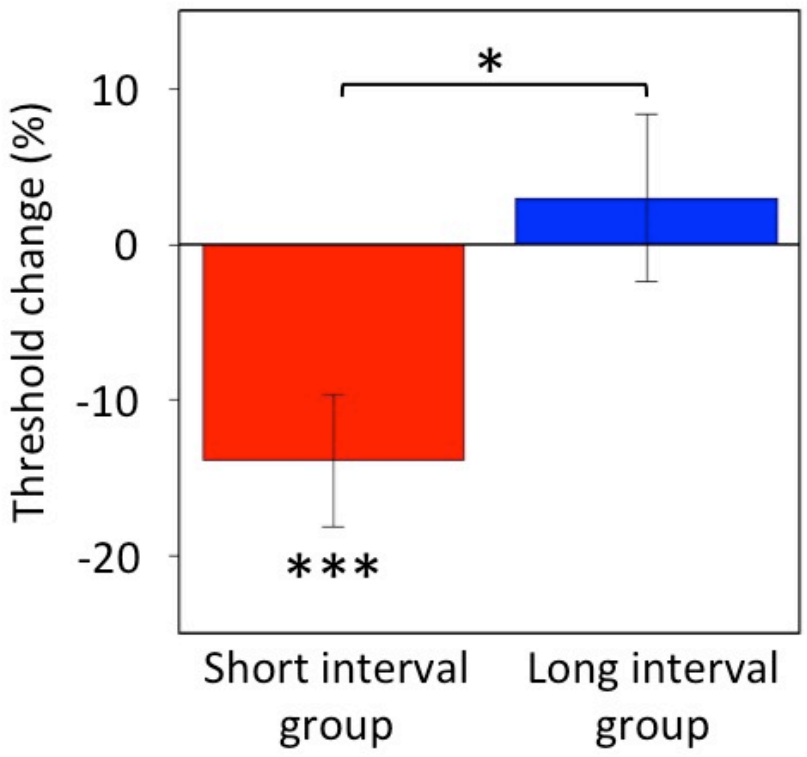

Figure 14. The performance change between day 2 and 3.

The threshold % change across day 2 and 3 for the short interval group (red) and long interval group (blue). Error bars are SEM (n=12). * p < 0.05, *** p < 0.005

4.2.3 Discussion

Our data suggests that reactivation makes previously consolidated VPL once again fragile, thus making it susceptible to interference from immediately following competing task. However, this reactivated VPL becomes stable again 3.5 hours after reactivation. This finding is consistent with previous findings from various memory domains. In the fear/motor and declarative memory, reactivated memory was impaired or its content was even modified when the reactivation was immediately followed by new learning (Chan & LaPaglia, 2013; Forcato et al., 2007; Hupbach et al., 2007; Schiller et al., 2010; Walker et al., 2003). In contrast, once the reactivated memory became

reconsolidated with a passage of time, new learning did not interfere with the reactivated memory (Nader, Schafe & Le Doux, 2000; Schiller et al., 2010; Seitz et al., 2005; Xue et al., 2012). The current study provides the first evidence showing that the reactivation and reconsolidation process also exists in VPL as in the other memory domains.

Nevertheless, the underlying neural mechanism of reactivation has not been well identified. Recently, it has been proposed that the E/I ratio directly regulates plastic potential of the brain (Bavelier et al., 2010; Hensch, 2005; Morishita & Hensch, 2008). Based on this, we investigated how E/I ratio in the early visual cortex is changed in association with reactivation in the following experiment.

4.3 E/I ratio change is associated with reactivation

4.3.1 Methods

4.3.1.1 Subjects

Twelve healthy subjects (6 males and 6 females, mean age 21 ± 2.37) with no use of medication participated in the experiment. All subjects had normal or corrected-to-normal vision and had no habit of playing video games. They kept regular wake and sleep pattern during experimental days. This study was approved by the Institutional Review Board of Brown University and all subjects gave written informed consents.

4.3.1.2 Experimental design

The purpose of this experiment was to investigate if the degree of plasticity of reactivated VPL is associated with changes in E/I ratio in the early visual cortex. The behavioral results indicated that previously consolidated VPL becomes fragile immediately after reactivation but becomes stable 3.5 hours after reactivation. Thus, we measured the E/I ratio in the early visual cortex before reactivation (pre-reactivation), shortly after reactivation (post-reactivation 1), and 3.5 hours after reactivation (post-reactivation 2) (see Chapter 2.3.1.2 for details).

This experiment consisted of three consecutive days and only one orientation (orientation A) was used (Figure 15). On the first day, subjects were given a brief test session of three blocks for initial threshold measurement. Then a training session consisting of 16 blocks was provided. Subjects performed this behavioral task inside a mock scanner that looks identical with 3T MR scanner. On the second day, subjects performed the same test session of three blocks inside 3T MR scanner and we had MRS scans immediately before, after and 3.5 hours after the test session. Please note that this test session served to reactivate previously consolidated VPL of orientation A. During the MRS scan, subjects performed a fixation task, in which central dot only was presented. Subjects were asked to detect a color change of the central dot by pressing a button. On the third day, the same test session of three blocks was conducted inside a mock scanner.

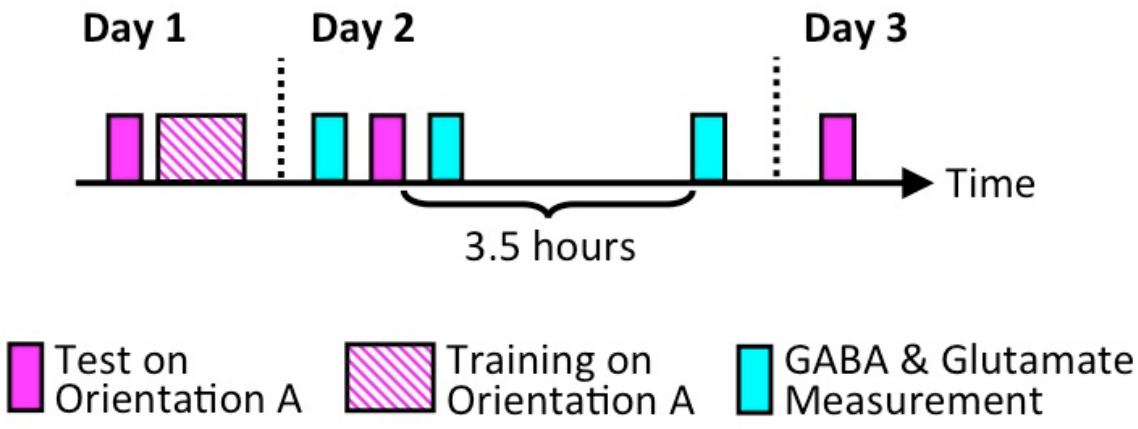

Figure 15. Experimental procedure.

4.3.1.3 Behavioral test and training sessions

The procedure of the behavioral test and training sessions was identical with that in the above behavioral experiment (Chapter 4.2.1.6).

4.3.1.4 Pre-reactivation, post-reactivation 1, and post-reactivation 2 sessions

Three MRS sessions were conducted in one day with the identical procedures. First, we obtained anatomical T1-weighted images. Second, based on the anatomical pictures, we positioned a voxel ($2 \times 2 \times 2cm^3$) manually along the calcarine sulcus so that the voxel covers the primary visual cortex. Third, an automatic shimming was performed by a vendor-provided automated shim tool. Then we manually performed a shimming to obtain the optimal shim value. This shim value was defined by a full width at half maximum of a water peak. The mean (± s.e.m) shim value across three sessions was 14.96 ± 0.31 Hz. These three steps took approximately 20-30 minutes. Finally, we

measured the concentration of GABA and glutamate from the voxel. GABA and glutamate scans took 774 and 384 sec, respectively. Please note that the pre-reactivation and post-reactivation 1 sessions were conducted in a row. Thus, we performed the first three steps of procedure only once at the beginning of the pre-reactivation session and the same parameters (voxel position and shim value) acquired from three steps in the pre-reactivation session were applied to the post-reactivation 1 session. At the beginning of the post-reactivation 2 session, we performed the first three steps again with delicate care so that the voxel covers the same region as in the pre-reactivation and post-reactivation 1 session.

During GABA and glutamate scans, subjects performed a fixation task, in which they were asked to fixate their eyes at the center of the screen and report the color change of the center dot by pressing a button in a key pad. A fixation dot was placed on a gray disk and the color of the dot changed from white ([R, G, B] = [255, 255, 255]) to faint pick ([R, G, B] = [255, 255 − x, 255 − x]) in an unpredictable way and returned to white 1.5 sec later. Initially, the color change x was set to 40 and controlled by 2-down 1-up staircase rule. If subjects pressed the button within 1.5 sec when the color of the dot changed, this response was regarded as hit. However, if subjects did not press the button within 1.5 sec when the color of the dot changed, it was regarded as miss. The geometric mean of the last 6 trials was taken as the threshold of the degree of color change x in each scan. To test if the thresholds changed across three sessions, we applied two-way repeated anova with session (pre-reactivation, post-reactivation 1, post-reactivation 2) and scan type (GABA, glutamate). The results indicated no significant effect of session ($F_{2,22} = 0.193$, $p = 0.826$), scan type ($F_{1,11} = 0.126$, $p = 0.729$), or interaction between

session and scan type ($F_{2,22} = 1.075$, $p = 0.359$). It suggests that subjects' performance at the fixation task remained stable across sessions and scan types.

4.3.1.5 MRI data acquisition

The procedure for MRI data acquisition was identical with that used in Chapter 2.3.1.5.

4.3.1.6 MRS data analysis

LC-model technique was used in all MRS data analysis. The underlying assumption of LC-model is that the obtained spectrum can be fitted in the frequency domain using a linear combination of basis functions. The Cramer-Rao Lower bounds indicate the reliability of quantification of GABA and glutamate. The mean (± s.e.m) Cramer-Rao lower bounds for GABA across participants was 6.64 ± 0.25 and that for glutamate was 4.64 ± 0.09, respectively. We normalized the amount of GABA and glutamate by using the amount of N-Acetylaspartate (NAA), which is a standard reference resonance (Provencher, 2001). Then we took the ratio of normalized amounts of glutamate to GABA as the E/I ratio per session. An E/I ratio at the pre-reactivation session was set to baseline individually. Then we calculated the E/I ratio change at each MRS session by using the equation:

$$E/I_{change}(t) = \left(\frac{Glu(t)/GABA(t)}{Glu(1)/GABA(1)} - 1\right) \times 100$$

Here, GABA(t) and Glu(t) represent the normalized concentrations of GABA and glutamate, respectively, at a certain MRS session t (1 = pre-reactivation, 2 = post-reactivation 1, 3 = post-reactivation 2).

4.3.2 Results

4.3.2.1 Behavioral results

Before examining the E/I ratio changes, we investigated if there has been any change in the performance of orientation detection task across three sessions. We expected to see the performance improvement between the first and the second day. The evidence of performance improvement would suggest that the learned orientation went through consolidation process. However, we did not expect any performance change between the second and the third day because there has been no training session on these days. We took the geometric mean of the last 6 reversals as a threshold S/N ratio per each block in the test session. Then, the geometric mean of the threshold S/N ratio across blocks was taken as the final threshold per subject.

We applied one-way repeated anova with day (day 1, day 2, day 3). The results indicated a significant effect of day ($F_{2,22} = 20.856$, $p < 0.005$, Figure 16). A Bonferroni post-hoc test showed that the threshold on the second day is significantly different from that on the first day, suggesting a performance improvement ($p = 0.001$). The threshold on the third day was also significantly different from that on the first day ($p = 0.003$), but the thresholds did not differ between the second and the third day ($p = 0.116$). The results suggest that improved performance did not change between the second and the third day.

From this, we can infer that the test session on the second day served as reactivation only, not as training.

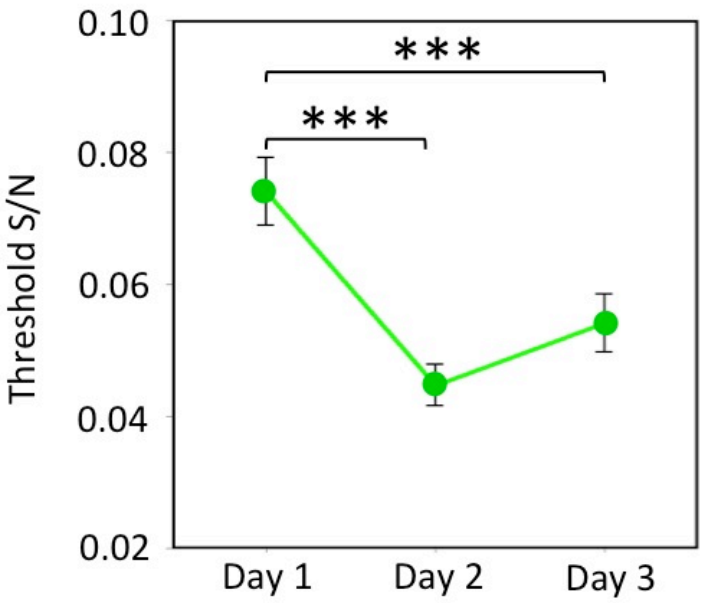

Figure 16. Threshold S/N ratio across three days. Error bars are SEM (n=12). *** p < 0.005

4.3.2.2 E/I ratio changes

To test if E/I ratio in the early visual cortex changes across three sessions, we calculated the E/I ratio changes at each session. The E/I ratio change was significantly greater than zero at post-reactivation 1 session, indicating that the E/I ratio increased immediately after reactivation compared to before reactivation (one sample 2-tailed t-test, $t(11) = 2.763$, $p = 0.018$, Figure 17). However, the E/I ratio change was not significantly different from zero at post-reactivation 2 session, suggesting that the E/I ratio at 3.5 hours after reactivation was not different from that before reactivation (one sample 2-tailed t-test, $t(11) = -0.154$, $p = 0.881$). Furthermore, we found a significant quadratic trend in E/I

ratio changes across three sessions ($F_{1,2} = 8.335$, $p = 0.015$). The results indicate that the E/I ratio increased immediately after reactivation but returned to the baseline 3.5 hours after reactivation.

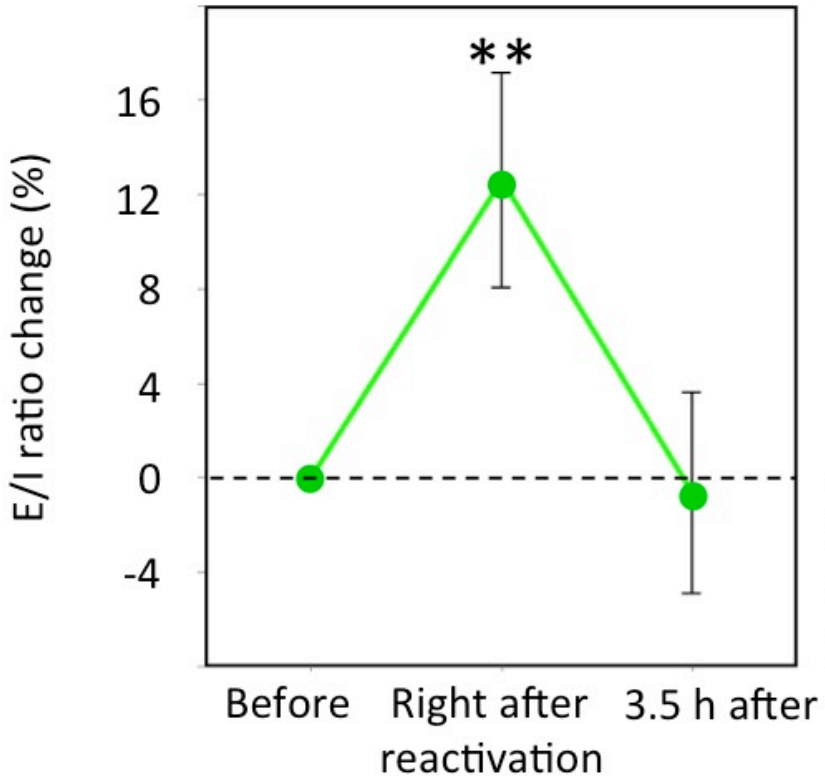

Figure 17. E/I ratio changes before, immediately after and 3.5 hours after reactivation. Error bars are SEM (n=12). ** p = 0.01

4.3.3 Discussion

In the current study, we found that the E/I ratio in the early visual cortex increases immediately after reactivation but decreases 3.5 hours after reactivation. Interestingly, the time interval where the E/I ratio increases matched the time interval where the reactivated VPL is interfered with by the following competing task. It suggests that the underlying

neural mechanism of reactivation is associated with the E/I ratio changes in the early visual cortex.

This result is in accord with previous finding in Chapter 2 in that the degree of plasticity in VPL is associated with the E/I ratio changes in the early visual cortex. Please note that the studies in Chapter 2 examined the association between plasticity in VPL with E/I ratio in the early visual cortex shortly after training and the current study in Chapter 4 examined this association immediately after reactivation. This line of evidence implies that the degree of plasticity in VPL may be governed by a common underlying mechanism, that is E/I ratio changes in the early visual cortex.

The current result also fits to the framework of developmental researches in which the onset and offset of the visual critical period is determined by the E/I ratio in the visual circuit (Bavelier et al., 2010; Hensch, 2005; Morishita & Hensch, 2008). Although the underlying neural mechanisms may not be exactly the same, the degree of plasticity of the visual system may be governed by a general process of E/I ratio changes in both critical period and adulthood.

Building on the findings in Chapter 4.2 and 4.3, we further questioned if the reactivation that we found in orientation detection task with gabor stimulus is a general process in VPL regardless of the task. To examine the possibility that the reactivation is a general process across various tasks, we tested if reactivation makes previously consolidated VPL fragile again against interference using TDT that is commonly used in VPL in the following experiment. Although testing TDT cannot guarantee that

reactivation is a general process in VPL, this new attempt can reveal a hint whether the reactivation process is observed beyond one specific task.

4.4 Possibility of generalization: Does reactivation process exists in TDT?

4.4.1 Methods

4.4.1.1 Subjects

Thirty healthy subjects (12 males and 18 females, mean age 19.64 ± 2.01) with no use of medication participated in the experiment. All subjects had normal or corrected-to-normal vision. They kept regular wake and sleep pattern during experimental days. All subjects were informed of the purpose and the procedures of the experiment and gave written informed consent, which was approved by the Institutional Review Board of Brown University where the experiment was conducted.

4.4.1.2 Experimental design

In the current experiment, we examined how reactivation affects stability of VPL in case of TDT, using two different background textures (Figure 7). The background of one TDT was filled with horizontal lines, whereas the other one was filled with vertical lines (Figure 18). These two background textures were selected as stimuli because they are known to interfere with each other when they are learned together within one hour (Yotsumoto et al., 2009a). We designated two different backgrounds of TDT either background A or B randomly for each subject. Additionally, we had two groups:

reactivation group and control group. The difference between these two groups was the presence of reactivation.

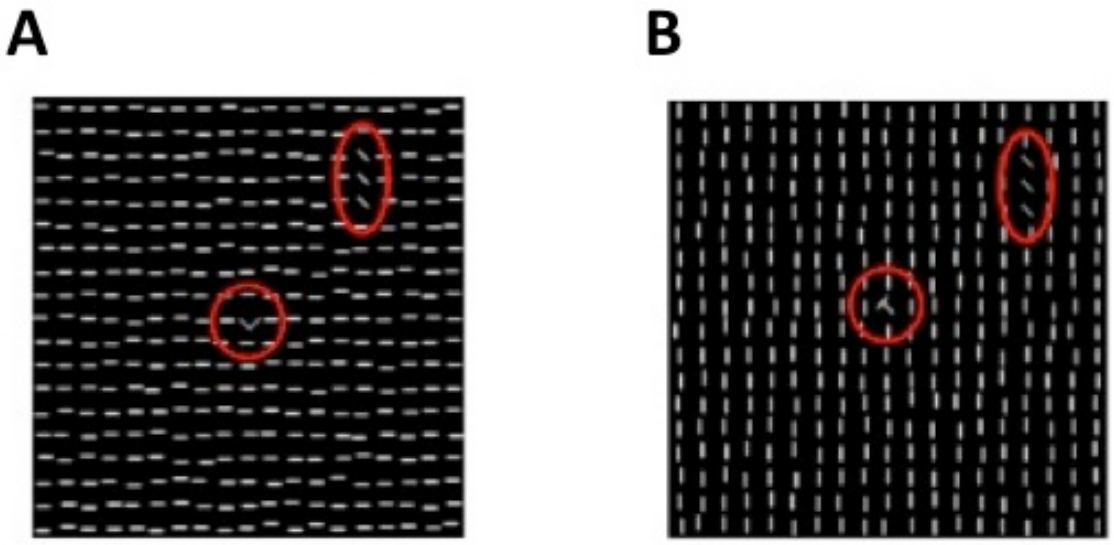

Figure 18. Two background textures used in TDT. (A) Background filled with horizontal lines. (B) Background filled with vertical lines.

The experiment consisted of three consecutive days (Figure 19). In the reactivation group, background A was trained on the first day, so that its VPL would be consolidated during subsequent wakefulness and sleep periods. On the second day, we reactivated the old VPL by giving subjects a brief test session of background A. Here, the test session served to reactivate the consolidated VPL. Details of the experimental parameters are shown in the next section. After the short test, another training of background B, which had different background texture was provided immediately. The purpose of background B training was to probe whether the reactivated VPL of background A was rendered vulnerable to interference. If reactivation returns VPL of

background A to a labile state, then background B should interfere with background A. In order to test this question, we provided another test sessions of background A and B on the third day.

The control group's experimental design was identical with that of group 1, except the reactivation via test session on the second day. In the control group, there was no test session of background A before training session of background B. Thus, there was no reactivation process in the control group.

If reactivation makes previously consolidated VPL of background A fragile against interference, we should observe a interference of background A by background B in the reactivation group only, but not in the control group. This interference effect can be observed by the comparison of the performance change on background A across the first and the third day between two groups. If the performance change on background A between the first and the third day is significantly lower in the reactivation group than that in the control group, it indicates that background B interfered with background A in the reactivation group.

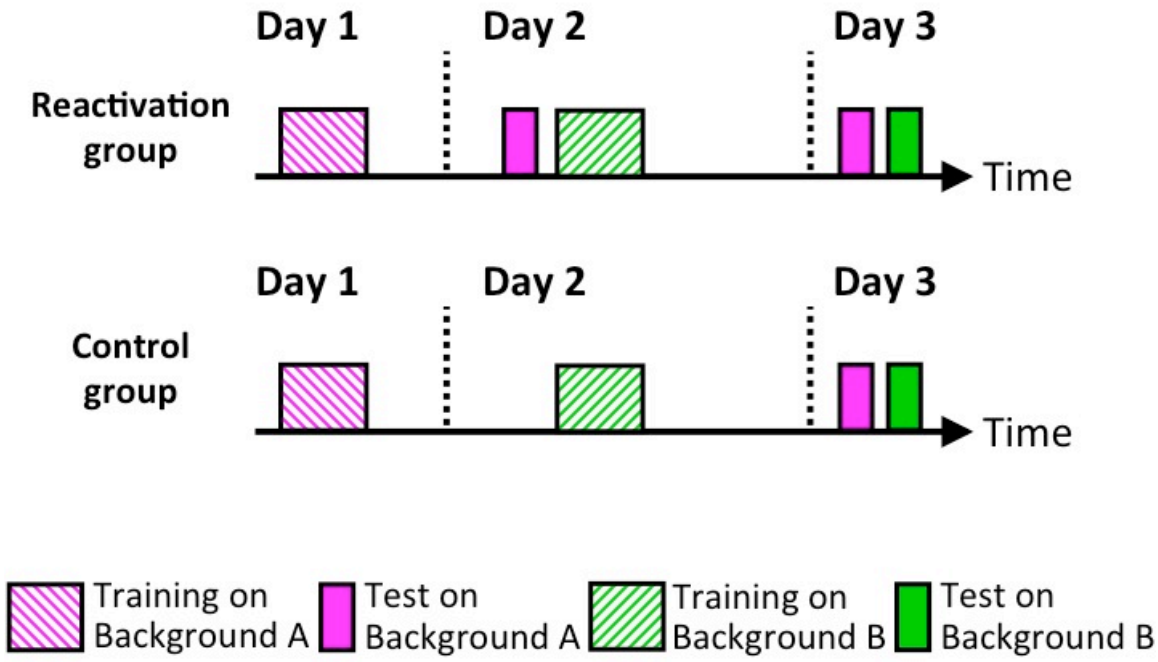

Figure 19. Experimental procedure

4.4.1.3 Texture discrimination task (TDT)

The task was identical with that used in the Chapter 3's behavioral experiment (Chapter 3.2.3).

4.4.1.4 Behavioral test and training sessions

In the behavioral test session of background A and B, subjects performed 140 trials of TDT with 7 SOAs (250, 200, 160, 140, 120, 100, 70 ms). The SOAs decreased sequentially. Each SOA was presented in one block with 20 trials. The test session took about five minutes.

During the training sessions of background A and B, subjects performed 420 trials of TDT with seven SOAs (250, 200, 160, 140, 120, 100, 70 ms). The training started with the longest SOA and decreased by every three blocks. Each block had 20 trials. The training session took approximately 20-25 minutes.

4.4.2 Results

4.4.2.1 Reactivation effect exists in TDT

To investigate whether reactivation makes previously consolidated VPL fragile again, we calculated the mean percentage of correctness in the three diagonal bars' task per each SOA. Then, we applied a logistic function to each individual's data to obtain the threshold SOA at 75% correctness. This fitting was done by using the psignifit toolbox (ver. 2.5.6) for Matlab (http://bootstrap-software.org/psignifit/). This toolbox package provides the maximum-likelihood method described by Wichmann and Hill (2001). Then, we calculated the normalized individual's threshold SOA change ratio between the first and the third days, by subtracting the 75% threshold SOA at the third day from that at the first day, and dividing it by that at the first day:

Threshold SOA change ratio = ((75% threshold SOA_{day1} – 75% threshold SOA_{day3}) / 75% threshold SOA_{day1}) × 100

The threshold change ratio was significantly lower in the reactivation group compared to that in the control group (2-tailed t-test, $t(28) = -2.531$, $p = 0.017$, Figure 20). It indicates that reactivation made background A labile against the interference from the

training of background B. The result is in accord with the previous finding in orientation detection task.

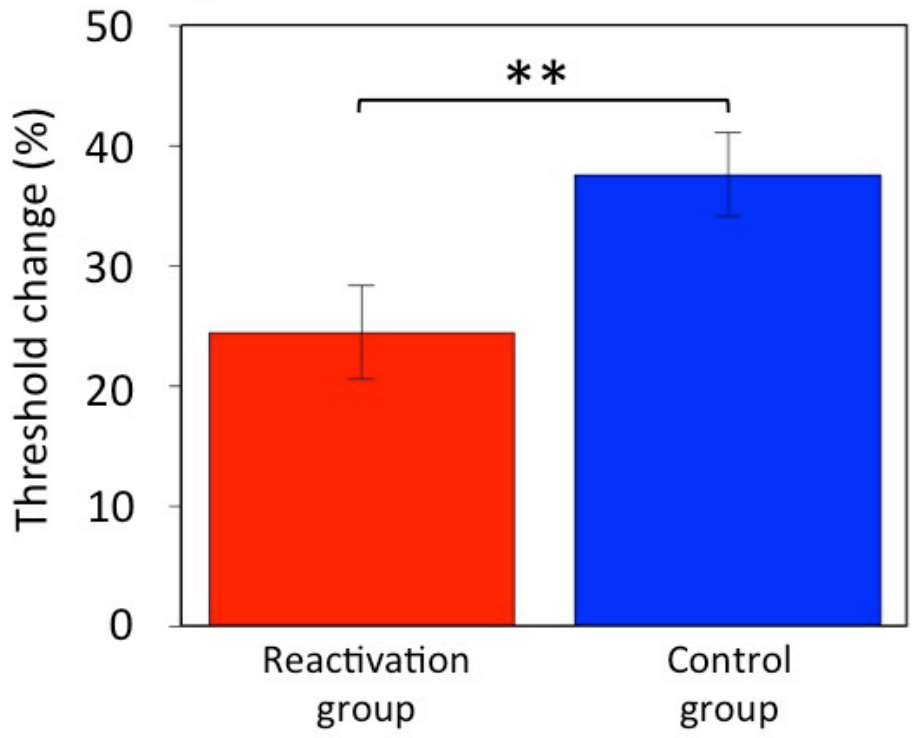

Figure 20. The performance change between day 1 and 3.

The threshold % change across day 1 and 3 for the reactivation group (red) and control group (blue). Error bars are SEM (n=15). ** p = 0.01

4.4.3 Discussion

Our data indicates that reactivation returns previously consolidated VPL fragile again, thus making it susceptible to interference in case of TDT. This result is consistent with our previous finding in orientation detection task (Chapter 4.2 & 4.3). Though our question about whether reactivation is a general process in VPL cannot be confirmed by

two experiments using orientation detection task and TDT, the current results suggest that the reactivation process is not limited to one specific task in VPL. Thus, the possibility that the reactivation is a general process in VPL is still a plausible and open question.

5. Chapter 5: Conclusion

The current study extends the knowledge about the temporal dynamics of plasticity in VPL. First, this dissertation work revealed the underlying neural mechanism of wake-dependent stabilization in VPL. Studies in Chapter 2 found that the E/I ratio changes in the early visual cortex are associated with the wake-dependent stabilization in VPL. When VPL is unstable, the E/I ratio is high, but when VPL is stable, the E/I ratio is low. It implies that the stability of VPL is governed by the E/I ratio changes in the early visual cortex.

Second, studies in Chapter 3 showed that slow sigma band activity corresponding to slow sleep spindles in the early visual cortex is involved in the sleep-dependent enhancement in VPL, at least in sleep stage 2 during the first sleep cycle. This finding favors the active system consolidation model, which claims that learned memory is actively replayed during subsequent sleep.

Third, my dissertation work showed that there are more temporal dynamics in VPL after wake-dependent and sleep-dependent consolidation processes after training. Results in Chapter 4 showed that even the previously consolidated VPL can become fragile once again when VPL is reactivated via a small number of trials. After the reactivation, VPL is unstable but becomes re-stabilized with a passage of time. This is the first study to show reactivation and reconsolidation processes in VPL.

Fourth, this work revealed the underlying neural mechanism of reactivation. Results in Chapter 4 demonstrated that the E/I ratio in the early visual cortex is changed in association with reactivation. When the reactivated VPL was put into a fragile state

against interference immediately after reactivation, the E/I ratio increased. In contrast, 3.5 hours after the reactivation, reactivated VPL became re-stabilized and the E/I ratio returned to the baseline. This finding is in accord with the finding in Chapter 2 and previous developmental studies, suggesting that the degree of plasticity in the visual system may be governed by the E/I ratio changes in the early visual cortex across the critical period and the adulthood.

In conclusion, my work focused on the temporal dynamics of VPL after training and revealed that learned VPL goes through dynamic processes even after the training is finished. The hope is that my dissertation work would stimulate the next future studies to reveal more about the dynamics of VPL.

References

Adab, H.Z., & Vogels, R. (2011). Practicing coarse orientation discrimination improves orientation signals in macaque cortical area v4. *Current Biology, 21* (19), 1661-1666.

Ahveninen, J., Lin, F.H., Kivisaari, R., Autti, T., Hamalainen, M., Stufflebeam, S., Belliveau, J.W., & Kahkonen, S. (2007). MRI-constrained spectral imaging of benzodiazepine modulation of spontaneous neuromagnetic activity in human cortex. *Neuroimage, 35* (2), 577-582.

Anderer, P., Klosch, G., Gruber, G., Trenker, E., Pascual-Marqui, R.D., Zeitlhofer, J., Barbanoj, M.J., Rappelsberger, P., & Saletu, B. (2001). Low-resolution brain electromagnetic tomography revealed simultaneously active frontal and parietal sleep spindle sources in the human cortex. *Neuroscience, 103* (3), 581-592.

Ball, K., & Sekuler, R. (1987). Direction-specific improvement in motion discrimination. *Vision Research, 27* (6), 953-965.

Bang, J.W., Khalilzadeh, O., Hamalainen, M., Watanabe, T., & Sasaki, Y. (2013). Location specific sleep spindle activity in the early visual areas and perceptual learning. *Vision Research,*

Barakat, M., Doyon, J., Debas, K., Vandewalle, G., Morin, A., Poirier, G., Martin, N., Lafortune, M., Karni, A., Ungerleider, L.G., Benali, H., & Carrier, J. (2011). Fast and slow spindle involvement in the consolidation of a new motor sequence. *Behavioural Brain Research, 217* (1), 117-121.

Bavelier, D., Levi, D.M., Li, R.W., Dan, Y., & Hensch, T.K. (2010). Removing brakes on adult brain plasticity: from molecular to behavioral interventions. *Journal of Neuroscience, 30* (45), 14964-14971.

Bergmann, T.O., Molle, M., Diedrichs, J., Born, J., & Siebner, H.R. (2012). Sleep spindle-related reactivation of category-specific cortical regions after learning face-scene associations. *Neuroimage, 59* (3), 2733-2742.

Born, J., Rasch, B., & Gais, S. (2006). Sleep to remember. *Neuroscientist, 12* (5), 410-424.

Born, J., & Wilhelm, I. (2012). System consolidation of memory during sleep. *Psychological Research, 76* (2), 192-203.

Buzsaki, G., & Draguhn, A. (2004). Neuronal oscillations in cortical networks. *Science, 304* (5679), 1926-1929.

Buzsaki, G., Haas, H.L., & Anderson, E.G. (1987). Long-Term Potentiation Induced by Physiologically Relevant Stimulus Patterns. *Brain Research, 435* (1-2), 331-333.

Censor, N., Karni, A., & Sagi, D. (2006). A link between perceptual learning, adaptation and sleep. *Vision Research, 46* (23), 4071-4074.

Censor, N., & Sagi, D. (2008). Benefits of efficient consolidation: short training enables long-term resistance to perceptual adaptation induced by intensive testing. *Vision Research, 48* (7), 970-977.

Chan, J.C.K., & LaPaglia, J.A. (2013). Impairing existing declarative memory in humans by disrupting reconsolidation. *Proceedings of the National Academy of Sciences of the United States of America, 110* (23), 9309-9313.

Chen, L., Yang, C., & Mower, G.D. (2001). Developmental changes in the expression of GABA(A) receptor subunits (alpha(1), alpha(2), alpha(3)) in the cat visual cortex and the effects of dark rearing. *Brain Research. Molecular Brain Research, 88* (1-2), 135-143.

Choi, H., Chang, L.H., Shibata, K., Sasaki, Y., & Watanabe, T. (2012). Resetting capacity limitations revealed by long-lasting elimination of attentional blink through training. *Proceedings of the National Academy of Sciences of the United States of America, 109* (30), 12242-12247.

Clark, V.P., Coffman, B.A., Mayer, A.R., Weisend, M.P., Lane, T.D.R., Calhoun, V.D., Raybourn, E.M., Garcia, C.M., & Wassermann, E.M. (2012). TDCS guided using fMRI significantly accelerates learning to identify concealed objects. *Neuroimage, 59* (1), 117-128.

Clark, V.P., Coffman, B.A., Trumbo, M.C., & Gasparovic, C. (2011). Transcranial direct current stimulation (tDCS) produces localized and specific alterations in neurochemistry: A H-1 magnetic resonance spectroscopy study. *Neuroscience Letters, 500* (1), 67-71.

Clemens, Z., Fabo, D., & Halasz, P. (2005). Overnight verbal memory retention correlates with the number of sleep spindles. *Neuroscience, 132* (2), 529-535.

Clemens, Z., Fabo, D., & Halasz, P. (2006). Twenty-four hours retention of visuospatial memory correlates with the number of parietal sleep spindles. *Neuroscience Letters, 403* (1-2), 52-56.

Cox, R.W., & Jesmanowicz, A. (1999). Real-time 3D image registration for functional MRI. *Magnetic Resonance in Medicine, 42* (6), 1014-1018.

Crist, R.E., Kapadia, M.K., Westheimer, G., & Gilbert, C.D. (1997). Perceptual learning of spatial localization: specificity for orientation, position, and context. *Journal of Neurophysiology, 78* (6), 2889-2894.

Czarnecki, A., Birtoli, B., & Ulrich, D. (2007). Cellular mechanisms of burst firing-mediated long-term depression in rat neocortical pyramidal cells. *J Physiol, 578* (Pt 2), 471-479.

Dale, A.M., Fischl, B., & Sereno, M.I. (1999). Cortical surface-based analysis. I. Segmentation and surface reconstruction. *Neuroimage, 9* (2), 179-194.

Dave, A.S., & Margoliash, D. (2000). Song replay during sleep and computational rules for sensorimotor vocal learning. *Science, 290* (5492), 812-816.

Davis, H.P., & Squire, L.R. (1984). Protein synthesis and memory: a review. *Psychological Bulletin, 96* (3), 518-559.

Engel, S.A., Rumelhart, D.E., Wandell, B.A., Lee, A.T., Glover, G.H., Chichilnisky, E.J., & Shadlen, M.N. (1994). fMRI of human visual cortex. *Nature, 369* (6481), 525.

Fagiolini, M., Fritschy, J.M., Low, K., Mohler, H., Rudolph, U., & Hensch, T.K. (2004). Specific GABA(A) circuits for visual cortical plasticity. *Science, 303* (5664), 1681-1683.

Fagiolini, M., & Hensch, T.K. (2000). Inhibitory threshold for critical-period activation in primary visual cortex. *Nature, 404* (6774), 183-186.

Fagiolini, M., Katagiri, H., Miyamoto, H., Mori, H., Grant, S.G., Mishina, M., & Hensch, T.K. (2003). Separable features of visual cortical plasticity revealed by N-methyl-D-aspartate receptor 2A signaling. *Proceedings of the National Academy of Sciences of the United States of America, 100* (5), 2854-2859.

Fahle, M., & Edelman, S. (1993). Long-term learning in vernier acuity: effects of stimulus orientation, range and of feedback. *Vision Research, 33* (3), 397-412.

Fiorentini, A., & Berardi, N. (1980). Perceptual learning specific for orientation and spatial frequency. *Nature, 287* (5777), 43-44.

Fischl, B., Sereno, M.I., & Dale, A.M. (1999). Cortical surface-based analysis. II: Inflation, flattening, and a surface-based coordinate system. *Neuroimage, 9* (2), 195-207.

Fize, D., Vanduffel, W., Nelissen, K., Denys, K., Chef d'Hotel, C., Faugeras, O., & Orban, G.A. (2003). The retinotopic organization of primate dorsal V4 and surrounding areas: A functional magnetic resonance imaging study in awake monkeys. *Journal of Neuroscience, 23* (19), 7395-7406.

Flexner, L.B., Flexner, J.B., & Stellar, E. (1965). Memory and cerebral protein synthesis in mice as affected by graded amounts of puromycin. *Experimental Neurology, 13* (3), 264-272.

Fogel, S.M., & Smith, C.T. (2006). Learning-dependent changes in sleep spindles and Stage 2 sleep. *Journal of Sleep Research, 15* (3), 250-255.

Forcato, C., Burgos, V.L., Argibay, P.F., Molina, V.A., Pedreira, M.E., & Maldonado, H. (2007). Reconsolidation of declarative memory in humans. *Learning and Memory, 14* (4), 295-303.

Gais, S., Molle, M., Helms, K., & Born, J. (2002). Learning-dependent increases in sleep spindle density. *Journal of Neuroscience, 22* (15), 6830-6834.

Gais, S., Plihal, W., Wagner, U., & Born, J. (2000). Early sleep triggers memory for early visual discrimination skills. *Nature Neuroscience, 3* (12), 1335-1339.

Goelet, P., Castellucci, V.F., Schacher, S., & Kandel, E.R. (1986). The long and the short of long-term memory--a molecular framework. *Nature, 322* (6078), 419-422.

Gu, Y., Fetsch, C.R., Adeyemo, B., Deangelis, G.C., & Angelaki, D.E. (2010). Decoding of MSTd population activity accounts for variations in the precision of heading perception. *Neuron, 66* (4), 596-609.

Hanover, J.L., Huang, Z.J., Tonegawa, S., & Stryker, M.P. (1999). Brain-derived neurotrophic factor overexpression induces precocious critical period in mouse visual cortex. *Journal of Neuroscience, 19* (22), art. no.-RC40.

Harauzov, A., Spolidoro, M., DiCristo, G., De Pasquale, R., Cancedda, L., Pizzorusso, T., Viegi, A., Berardi, N., & Maffei, L. (2010). Reducing intracortical inhibition in the adult visual cortex promotes ocular dominance plasticity. *Journal of Neuroscience, 30* (1), 361-371.

Harris, H., Gliksberg, M., & Sagi, D. (2012). Generalized perceptual learning in the absence of sensory adaptation. *Current Biology, 22* (19), 1813-1817.

Hasselmo, M.E. (1999). Neuromodulation: acetylcholine and memory consolidation. *Trends Cogn Sci, 3* (9), 351-359.

He, H.Y., Ray, B., Dennis, K., & Quinlan, E.M. (2007). Experience-dependent recovery of vision following chronic deprivation amblyopia. *Nature Neuroscience, 10* (9), 1134-1136.

Hensch, T.K. (2005). Critical period plasticity in local cortical circuits. *Nat Rev Neurosci, 6* (11), 877-888.

Hensch, T.K., Fagiolini, M., Mataga, N., Stryker, M.P., Baekkeskov, S., & Kash, S.F. (1998). Local GABA circuit control of experience-dependent plasticity in developing visual cortex. *Science, 282* (5393), 1504-1508.

Hoddes, E., Zarcone, V., Smythe, H., Phillips, R., & Dement, W.C. (1973). Quantification of sleepiness: a new approach. *Psychophysiology, 10* (4), 431-436.

Hua, T., Bao, P., Huang, C.B., Wang, Z., Xu, J., Zhou, Y., & Lu, Z.L. (2010). Perceptual learning improves contrast sensitivity of V1 neurons in cats. *Current Biology, 20* (10), 887-894.

Huang, C.B., Lu, Z.L., & Dosher, B.A. (2012). Co-learning analysis of two perceptual learning tasks with identical input stimuli supports the reweighting hypothesis. *Vision Research, 61*, 25-32.

Huang, Z.J., Kirkwood, A., Pizzorusso, T., Porciatti, V., Morales, B., Bear, M.F., Maffei, L., & Tonegawa, S. (1999). BDNF regulates the maturation of inhibition and the critical period of plasticity in mouse visual cortex. *Cell, 98* (6), 739-755.

Hubel, D.H., & Wiesel, T.N. (1970). The period of susceptibility to the physiological effects of unilateral eye closure in kittens. *J Physiol, 206* (2), 419-436.

Huber, R., Ghilardi, M.F., Massimini, M., Ferrarelli, F., Riedner, B.A., Peterson, M.J., & Tononi, G. (2006). Arm immobilization causes cortical plastic changes and locally decreases sleep slow wave activity. *Nature Neuroscience, 9* (9), 1169-1176.

Huber, R., Ghilardi, M.F., Massimini, M., & Tononi, G. (2004). Local sleep and learning. *Nature, 430* (6995), 78-81.

Hupbach, A., Gomez, R., Hardt, O., & Nadel, L. (2007). Reconsolidation of episodic memories: a subtle reminder triggers integration of new information. *Learning and Memory, 14* (1-2), 47-53.

Iber, C. (2007). The AASM manual for the scoring of sleep and associated events: rules, terminology and technical specifications. (American Academy of Sleep Medicine.

Iwai, Y., Fagiolini, M., Obata, K., & Hensch, T.K. (2003). Rapid critical period induction by tonic inhibition in visual cortex. *Journal of Neuroscience, 23* (17), 6695-6702.

Ji, D., & Wilson, M.A. (2007). Coordinated memory replay in the visual cortex and hippocampus during sleep. *Nature Neuroscience, 10* (1), 100-107.

Karni, A., & Sagi, D. (1991). Where practice makes perfect in texture discrimination: evidence for primary visual cortex plasticity. *Proceedings of the National Academy of Sciences of the United States of America, 88* (11), 4966-4970.

Karni, A., & Sagi, D. (1993). The time course of learning a visual skill. *Nature, 365* (6443), 250-252.

Karni, A., Tanne, D., Rubenstein, B.S., Askenasy, J.J.M., & Sagi, D. (1994). Dependence on Rem-Sleep of Overnight Improvement of a Perceptual Skill. *Science, 265* (5172), 679-682.

Kim, S., Stephenson, M.C., Morris, P.G., & Jackson, S.R. (2014). tDCS-induced alterations in GABA concentration within primary motor cortex predict motor learning and motor memory: A 7 T magnetic resonance spectroscopy study. *Neuroimage, 99*, 237-243.

King, C., Henze, D.A., Leinekugel, X., & Buzsaki, G. (1999). Hebbian modification of a hippocampal population pattern in the rat. *J Physiol, 521 Pt 1*, 159-167.

Korman, M., Doyon, J., Doljansky, J., Carrier, J., Dagan, Y., & Karni, A. (2007). Daytime sleep condenses the time course of motor memory consolidation. *Nature Neuroscience, 10* (9), 1206-1213.

Koyama, S., Harner, A., & Watanabe, T. (2004). Task-dependent changes of the psychophysical motion-tuning functions in the course of perceptual learning. *Perception, 33* (9), 1139-1147.

Law, C.T., & Gold, J.I. (2008). Neural correlates of perceptual learning in a sensory-motor, but not a sensory, cortical area. *Nature Neuroscience, 11* (4), 505-513.

Lewis, T.L., & Maurer, D. (2009). Effects of early pattern deprivation on visual development. *Optometry and Vision Science, 86* (6), 640-646.

Li, W., Piech, V., & Gilbert, C.D. (2004). Perceptual learning and top-down influences in primary visual cortex. *Nature Neuroscience, 7* (6), 651-657.

Lin, F.H., Witzel, T., Hamalainen, M.S., Dale, A.M., Belliveau, J.W., & Stufflebeam, S.M. (2004). Spectral spatiotemporal imaging of cortical oscillations and interactions in the human brain. *Neuroimage, 23* (2), 582-595.

Lu, Z.L., Hua, T.M., Huang, C.B., Zhou, Y.F., & Dosher, B.A. (2011). Visual perceptual learning. *Neurobiology of Learning and Memory, 95* (2), 145-151.

Margoliash, D. (2010). Sleep, learning, and birdsong. *ILAR J, 51* (4), 378-386.

Maya-Vetencourt, J.F., Sale, A., Viegi, A., Baroncelli, L., De Pasquale, R., O'Leary, O.F., Castren, E., & Maffei, L. (2008). The antidepressant fluoxetine restores plasticity in the adult visual cortex. *Science, 320* (5874), 385-388.

McGaugh, J.L. (2000). Memory--a century of consolidation. *Science, 287* (5451), 248-251.

McKee, S.P., & Westheimer, G. (1978). Improvement in vernier acuity with practice. *Perception and Psychophysics, 24* (3), 258-262.

Mednick, S., Nakayama, K., & Stickgold, R. (2003). Sleep-dependent learning: a nap is as good as a night. *Nature Neuroscience, 6* (7), 697-698.

Mednick, S.C., Arman, A.C., & Boynton, G.M. (2005). The time course and specificity of perceptual deterioration. *Proceedings of the National Academy of Sciences of the United States of America, 102* (10), 3881-3885.

Mednick, S.C., McDevitt, E.A., Walsh, J.K., Wamsley, E., Paulus, M., Kanady, J.C., & Drummond, S.P. (2013). The critical role of sleep spindles in hippocampal-dependent memory: a pharmacology study. *Journal of Neuroscience, 33* (10), 4494-4504.

Mednick, S.C., Nakayama, K., Cantero, J.L., Atienza, M., Levin, A.A., Pathak, N., & Stickgold, R. (2002). The restorative effect of naps on perceptual deterioration. *Nature Neuroscience, 5* (7), 677-681.

Molle, M., Eschenko, O., Gais, S., Sara, S.J., & Born, J. (2009). The influence of learning on sleep slow oscillations and associated spindles and ripples in humans and rats. *European Journal of Neuroscience, 29* (5), 1071-1081.

Montey, K.L., & Quinlan, E.M. (2011). Recovery from chronic monocular deprivation following reactivation of thalamocortical plasticity by dark exposure. *Nat Commun, 2*, 317.

Morales, B., Choi, S.Y., & Kirkwood, A. (2002). Dark rearing alters the development of GABAergic transmission in visual cortex. *Journal of Neuroscience, 22* (18), 8084-8090.

Morin, A., Doyon, J., Dostie, V., Barakat, M., Hadj Tahar, A., Korman, M., Benali, H., Karni, A., Ungerleider, L.G., & Carrier, J. (2008). Motor sequence learning increases sleep spindles and fast frequencies in post-training sleep. *Sleep, 31* (8), 1149-1156.

Morishita, H., & Hensch, T.K. (2008). Critical period revisited: impact on vision. *Curr Opin Neurobiol, 18* (1), 101-107.

Mower, G.D. (1991). The effect of dark rearing on the time course of the critical period in cat visual cortex. *Brain Research. Developmental Brain Research, 58* (2), 151-158.

Nader, K., Schafe, G.E., & Le Doux, J.E. (2000). Fear memories require protein synthesis in the amygdala for reconsolidation after retrieval. *Nature, 406* (6797), 722-726.

Nishida, M., & Walker, M.P. (2007). Daytime Naps, Motor Memory Consolidation and Regionally Specific Sleep Spindles. *Plos One, 2* (4)

Peigneux, P., Laureys, S., Fuchs, S., Collette, F., Perrin, F., Reggers, J., Phillips, C., Degueldre, C., Del Fiore, G., Aerts, J., Luxen, A., & Maquet, P. (2004). Are spatial memories strengthened in the human hippocampus during slow wave sleep? *Neuron, 44* (3), 535-545.

Petrov, A.A., Dosher, B.A., & Lu, Z.L. (2006). Perceptual learning without feedback in non-stationary contexts: Data and model. *Vision Research, 46* (19), 3177-3197.

Poggio, T., Fahle, M., & Edelman, S. (1992). Fast perceptual learning in visual hyperacuity. *Science, 256* (5059), 1018-1021.

Provencher, S.W. (2001). Automatic quantitation of localized in vivo 1H spectra with LCModel. *NMR in Biomedicine, 14* (4), 260-264.

Raiguel, S., Vogels, R., Mysore, S.G., & Orban, G.A. (2006). Learning to see the difference specifically alters the most informative V4 neurons. *Journal of Neuroscience, 26* (24), 6589-6602.

Rasch, B., Buchel, C., Gais, S., & Born, J. (2007). Odor cues during slow-wave sleep prompt declarative memory consolidation. *Science, 315* (5817), 1426-1429.

Rosanova, M., & Ulrich, D. (2005). Pattern-specific associative long-term potentiation induced by a sleep spindle-related spike train. *Journal of Neuroscience, 25* (41), 9398-9405.

Sagi, D. (2011). Perceptual learning in Vision Research. *Vision Research, 51* (13), 1552-1566.

Sagi, D., & Tanne, D. (1994). Perceptual learning: learning to see. *Current Opinion in Neurobiology, 4* (2), 195-199.

Sale, A., Maya Vetencourt, J.F., Medini, P., Cenni, M.C., Baroncelli, L., De Pasquale, R., & Maffei, L. (2007). Environmental enrichment in adulthood promotes amblyopia recovery through a reduction of intracortical inhibition. *Nature Neuroscience, 10* (6), 679-681.

Sasaki, Y., Nanez, J.E., & Watanabe, T. (2010). Advances in visual perceptual learning and plasticity. *Nat Rev Neurosci, 11* (1), 53-60.

Schabus, M., Dang-Vu, T.T., Albouy, G., Balteau, E., Boly, M., Carrier, J., Darsaud, A., Degueldre, C., Desseilles, M., Gais, S., Phillips, C., Rauchs, G., Schnakers, C., Sterpenich, V., Vandewalle, G., Luxen, A., & Maquet, P. (2007). Hemodynamic cerebral correlates of sleep spindles during human non-rapid eye movement sleep. *Proceedings of the National Academy of Sciences of the United States of America, 104* (32), 13164-13169.

Schabus, M., Gruber, G., Parapatics, S., Sauter, C., Klosch, G., Anderer, P., Klimesch, W., Saletu, B., & Zeitlhofer, J. (2004). Sleep spindles and their significance for declarative memory consolidation. *Sleep, 27* (8), 1479-1485.

Schiller, D., Monfils, M.H., Raio, C.M., Johnson, D.C., LeDoux, J.E., & Phelps, E.A. (2010). Preventing the return of fear in humans using reconsolidation update mechanisms. *Nature, 463* (7277), 49-U51.

Schmidt, C., Peigneux, P., Muto, V., Schenkel, M., Knoblauch, V., Munch, M., de Quervain, D.J., Wirz-Justice, A., & Cajochen, C. (2006). Encoding difficulty promotes postlearning changes in sleep spindle activity during napping. *Journal of Neuroscience, 26* (35), 8976-8982.

Schoups, A., Vogels, R., Qian, N., & Orban, G. (2001). Practising orientation identification improves orientation coding in V1 neurons. *Nature, 412* (6846), 549-553.

Schwartz, S., Maquet, P., & Frith, C. (2002). Neural correlates of perceptual learning: a functional MRI study of visual texture discrimination. *Proceedings of the National Academy of Sciences of the United States of America, 99* (26), 17137-17142.

Seitz, A.R., Yamagishi, N., Werner, B., Goda, N., Kawato, M., & Watanabe, T. (2005). Task-specific disruption of perceptual learning. *Proceedings of the National Academy of Sciences of the United States of America, 102* (41), 14895-14900.

Sereno, M.I., Dale, A.M., Reppas, J.B., Kwong, K.K., Belliveau, J.W., Brady, T.J., Rosen, B.R., & Tootell, R.B. (1995). Borders of multiple visual areas in humans revealed by functional magnetic resonance imaging. *Science, 268* (5212), 889-893.

Shibata, K., Chang, L.H., Kim, D., Nanez, J.E., Sr., Kamitani, Y., Watanabe, T., & Sasaki, Y. (2012). Decoding reveals plasticity in V3A as a result of motion perceptual learning. *Plos One, 7* (8), e44003.

Shibata, K., Watanabe, T., Sasaki, Y., & Kawato, M. (2011). Perceptual learning incepted by decoded fMRI neurofeedback without stimulus presentation. *Science, 334* (6061), 1413-1415.

Shiu, L.P., & Pashler, H. (1992). Improvement in line orientation discrimination is retinally local but dependent on cognitive set. *Perception and Psychophysics, 52* (5), 582-588.

Squire, L.R., & Davis, H.P. (1981). The pharmacology of memory: a neurobiological perspective. *Annual Review of Pharmacology and Toxicology, 21*, 323-356.

Stagg, C.J., Bachtiar, V., & Johansen-Berg, H. (2011). The Role of GABA in Human Motor Learning. *Current Biology, 21* (6), 480-484.

Steriade, M. (1999). Coherent oscillations and short-term plasticity in corticothalamic networks. *Trends in Neurosciences, 22* (8), 337-345.

Steriade, M. (2006). Grouping of brain rhythms in corticothalamic systems. *Neuroscience, 137* (4), 1087-1106.

Steriade, M., McCormick, D.A., & Sejnowski, T.J. (1993). Thalamocortical oscillations in the sleeping and aroused brain. *Science, 262* (5134), 679-685.

Stickgold, R., James, L., & Hobson, J.A. (2000). Visual discrimination learning requires sleep after training. *Nature Neuroscience, 3* (12), 1237-1238.

Stickgold, R., Whidbee, D., Schirmer, B., Patel, V., & Hobson, J.A. (2000). Visual discrimination task improvement: A multi-step process occurring during sleep. *Journal of Cognitive Neuroscience, 12* (2), 246-254.

Tamaki, M., Huang, T.R., Yotsumoto, Y., Hamalainen, M., Lin, F.H., Nanez, J.E., Sr., Watanabe, T., & Sasaki, Y. (2013). Enhanced spontaneous oscillations in the supplementary motor area are associated with sleep-dependent offline learning of finger-tapping motor-sequence task. *Journal of Neuroscience, 33* (34), 13894-13902.

Tamaki, M., Matsuoka, T., Nittono, H., & Hori, T. (2008). Fast sleep spindle (13-15 hz) activity correlates with sleep-dependent improvement in visuomotor performance. *Sleep, 31* (2), 204-211.

Tamaki, M., Matsuoka, T., Nittono, H., & Hori, T. (2009). Activation of fast sleep spindles at the premotor cortex and parietal areas contributes to motor learning: a study using sLORETA. *Clinical Neurophysiology, 120* (5), 878-886.

Tamaki, M., Nittono, H., Hayashi, M., & Hori, T. (2005). Examination of the first-night effect during the sleep-onset period. *Sleep, 28* (2), 195-202.

Tononi, G., & Cirelli, C. (2003). Sleep and synaptic homeostasis: a hypothesis. *Brain Research Bulletin, 62* (2), 143-150.

Tononi, G., & Cirelli, C. (2006). Sleep function and synaptic homeostasis. *Sleep Med Rev, 10* (1), 49-62.

Uutela, K., Taulu, S., & Hamalainen, M. (2001). Detecting and correcting for head movements in neuromagnetic measurements. *Neuroimage, 14* (6), 1424-1431.

Vaina, L.M., Belliveau, J.W., des Roziers, E.B., & Zeffiro, T.A. (1998). Neural systems underlying learning and representation of global motion. *Proceedings of the National Academy of Sciences of the United States of America, 95* (21), 12657-12662.

Walker, M.P., Brakefield, T., Hobson, J.A., & Stickgold, R. (2003). Dissociable stages of human memory consolidation and reconsolidation. *Nature, 425* (6958), 616-620.

Walker, M.P., Stickgold, R., Jolesz, F.A., & Yoo, S.S. (2005). The functional anatomy of sleep-dependent visual skill learning. *Cerebral Cortex, 15* (11), 1666-1675.

Wamsley, E.J., Tucker, M.A., Shinn, A.K., Ono, K.E., McKinley, S.K., Ely, A.V., Goff, D.C., Stickgold, R., & Manoach, D.S. (2012). Reduced sleep spindles and spindle coherence in schizophrenia: mechanisms of impaired memory consolidation? *Biological Psychiatry, 71* (2), 154-161.

Watanabe, T., Nanez, J.E., Koyama, S., Mukai, I., Liederman, J., & Sasaki, Y. (2002). Greater plasticity in lower-level than higher-level visual motion processing in a passive perceptual learning task. *Nature Neuroscience, 5* (10), 1003-1009.

Werth, E., Achermann, P., Dijk, D.J., & Borbely, A.A. (1997). Spindle frequency activity in the sleep EEG: individual differences and topographic distribution. *Electroencephalography and Clinical Neurophysiology, 103* (5), 535-542.

Wichmann, F.A., & Hill, N.J. (2001). The psychometric function: I. Fitting, sampling, and goodness of fit. *Perception and Psychophysics, 63* (8), 1293-1313.

Wilson, M.A., & McNaughton, B.L. (1994). Reactivation of hippocampal ensemble memories during sleep. *Science, 265* (5172), 676-679.

Xiao, L.Q., Zhang, J.Y., Wang, R., Klein, S.A., Levi, D.M., & Yu, C. (2008). Complete transfer of perceptual learning across retinal locations enabled by double training. *Current Biology, 18* (24), 1922-1926.

Xue, Y.X., Luo, Y.X., Wu, P., Shi, H.S., Xue, L.F., Chen, C., Zhu, W.L., Ding, Z.B., Bao, Y.P., Shi, J., Epstein, D.H., Shaham, Y., & Lu, L. (2012). A memory retrieval-extinction procedure to prevent drug craving and relapse. *Science, 336* (6078), 241-245.

Yang, T., & Maunsell, J.H. (2004). The effect of perceptual learning on neuronal responses in monkey visual area V4. *Journal of Neuroscience, 24* (7), 1617-1626.

Yotsumoto, Y., Chang, L.H., Watanabe, T., & Sasaki, Y. (2009a). Interference and feature specificity in visual perceptual learning. *Vision Research, 49* (21), 2611-2623.

Yotsumoto, Y., Sasaki, Y., Chan, P., Vasios, C.E., Bonmassar, G., Ito, N., Nanez, J.E., Sr., Shimojo, S., & Watanabe, T. (2009b). Location-specific cortical activation changes during sleep after training for perceptual learning. *Current Biology, 19* (15), 1278-1282.

Yotsumoto, Y., Watanabe, T., & Sasaki, Y. (2008). Different dynamics of performance and brain activation in the time course of perceptual learning. *Neuron, 57* (6), 827-833.

Zeitlhofer, J., Gruber, G., Anderer, P., Asenbaum, S., Schimicek, P., & Saletu, B. (1997). Topographic distribution of sleep spindles in young healthy subjects. *Journal of Sleep Research, 6* (3), 149-155.

Zhang, J.Y., Zhang, G.L., Xiao, L.Q., Klein, S.A., Levi, D.M., & Yu, C. (2010a). Rule-based learning explains visual perceptual learning and its specificity and transfer. *Journal of Neuroscience, 30* (37), 12323-12328.

Zhang, T., Xiao, L.Q., Klein, S.A., Levi, D.M., & Yu, C. (2010b). Decoupling location specificity from perceptual learning of orientation discrimination. *Vision Research, 50* (4), 368-374.

Zohary, E., Celebrini, S., Britten, K.H., & Newsome, W.T. (1994). Neuronal Plasticity That Underlies Improvement in Perceptual Performance. *Science, 263* (5151), 1289-1292.